CHAPTER ONE

Development of methylene blue-loaded polyhydroxybutyrate nanofibers for biomedical applications

1. Introduction

Polymeric nanofibrous systems represent a unique group of materials that have recently gained widespread interest in tissue engineering and drug delivery applications [229, 230]. As cell regenerative and tissue engineering platforms, nanofibrous membranes/scaffolds possess three-dimensional nanosized mesh structures that closely resemble that of the native extracellular matrix. Their high surface area-to-volume ratio also enables enhancement of cellular attachment and efficient mass transport from the scaffolds. Electrospun nanofibers have shown a great potential in the engineering of a number of tissues including vasculature [231], bone [232, 233], neural and tendon/ligament tissues [234, 235], and skin [236]. Flexible modulation of the electrospinning process parameters allows the control of fiber alignment and porosity as needed for each application [237].

Different polymers can be spun into nanofibers by the electrospinning of natural [40, 41, 132, 141] and synthetic polymers [238-240] including aliphatic polyesters such as poly (lactic-co-glycolic acid) (PLGA) [130], poly (1-caprolactone) (PCL) [33] and polyhydroxyalkanoate as polyhydroxybutyrate (PHB) [241] and polyhydroxybutyrate-co-valerate (PHBV) [242]. Polyhydroxyalkanoates (PHAs) are hydrophobic biopolyesters produced by a range of microorganisms [243]. Polyhydroxybutyrate (PHB), which is widely used as a biomaterial in medical implantation devices [244] is the most commonly studied polymers among the PHAs. PHB an FDA approved product that is both biocompatible and biodegradable. PHB has ideal compatibility, in part as a consequence of its natural presence in mammalian blood and tissues [245]. Moreover its constituent monomeric unit, hydroxybutyric acid, is one of the ketone bodies, a native compound in mammals produced during diabetes and prolonged starvation [246]. However, due to its brittle nature, slow *in vivo* degradation and relative high manufacturing costs, applications of PHB are restricted. One strategy to overcome PHB impediments is copolymerization with a valerate unit (PHBV) or by blending with other biopolymers such as polyvinyl alcohol PVA and polyethylene glycol (PEG). Such a strategy leads to improved material properties by increasing hydrophilicity, reducing crystallinity, promoting degradation under physiological conditions and reducing costs [247-249].

Functionality of nanofibrous membranes/scaffolds can be further enhanced by loading with various therapeutic molecules aiming to boost their bioactivity or overcome untoward bio-responses. Loaded therapeutics encompass among others, specific growth factors, morphogens and proteins to stimulate cellular adhesion, proliferation and differentiation [250], anti-inflammatory drugs [251] and anti-resorption agents such as bisphosphonates in bone tissue engineering [252].

NFs with antimicrobial functionality are attracting growing attention as a biomaterial platform for infection control and prophylactic and therapeutic applications. For instance, NFs made of antimicrobial polymers have been used for the engineering of protective face masks [253], antimicrobial textiles [227], self-disinfecting surfaces [254] and implantable medical devices [255]. Among other prophylactic applications, NFs were assessed for the prevention of osteomyelitis [256] post-surgical tissue adhesions [130] and the infection of wounds [257].

For the therapeutic treatment of infected wounds, NFs loaded with diverse antimicrobial agents have been the subject of extensive research as multifunctional drug delivery scaffolds capable of enhancing wound cellular repair and controlling infection [257]. In this context, NFs have been mainly functionalized with antibiotics such as cefoxitin sodium [30] and fusidic acid [257] and nanobiocides, mainly silver nanoparticles [258]. These NFs matrices showed in vitro antimicrobial activity and wound healing accelerating effects in animal models.

In addition to antibiotics, incorporation of antibacterial agents and antiseptics such iodine-polymer complexes [85], triclosan [259], chlorhexidine [260] and polyhexamethylene biguanide [261] in electrospun matrices have been the subject of several reports. Despite antimicrobial effectiveness, concerns could be raised regarding possible antimicrobial resistance to antibiotics and silver nanoparticles in addition to systemic toxicity [262, 263].

Antiseptic dye-loaded dressings could provide an alternative to overcome at least some limitations of other antimicrobials/antibiotics and broaden clinical diversity of local therapeutics. The use of antiseptic dyes including acridine, triphenylmethane and phenothiazine dyes against bacterial and fungal infections saved many lives. For example, during the First World War, flavine therapy was employed in battlefield injuries and agents such as the acridine dye, acriflavine, were also tested as systemic (oral) preparations for gonorrhea [264]. Although the use of antiseptic dyes has been reduced by the emergence of antibiotics and because of tissue staining, they could be reconsidered in the era of antimicrobial resistance to conserve more valuable agents for systemic chemotherapy. Bacteriostatic wound dressings impregnated with antiseptic dyes providing a broad spectrum of activity against microorganisms commonly found in wounds, including methicillin-resistant Staphylococcus aureus (MRSA) and vancomycin-resistant Enterococcus (VRE) are available commercially [263].

Methylene blue (MB), a phenothiazine dye, is a cationic soluble dye [265]. It has a recognized antimicrobial effect in the dark which can be potentiated in oxygenated environment, through photoactivation by light with a wavelength corresponding to its electronic absorption band, which leads to the production of reactive singlet oxygen species and/or free radicals capable of destroying both prokaryotic and eukaryotic cells [266, 267]. Bioactivity of methylene blue also extends to antioxidant and anti-tissue adhesion effects [268-271]. Therefore, MB loaded delivery systems would find widespread biomedical application potentials.

The objective of chapter 1 of the thesis was to develop controlled delivery MB-eluting PHB-based NFs combining the advantage of NFs as a multifunctional matrix with temporal control on MB delivery (which prolongs the action of MB at the application site, enhancing its activity) and those of MB as a dye with multiple biological effects. These NFs offer potentials as a MB-eluting scaffold delivery system for biomedical applications involving the diverse biological activities of MB such as antimicrobial, antioxidant, photosensitizing and other activities.

2. Materials and Methods

2.1. Chemicals

- **Methylene blue (MB),** Mw 373.9 (Aldrich chemical co. Ltd., England)
  - Chemical structure

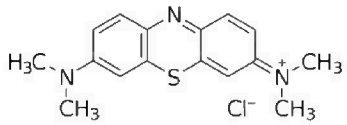

  - Chemical Formula: $C_{16}H_{18}ClN_3S$.
  - IUPAC-Name: 3,7-bis(Dimethylamino)-phenothiazin-5-ium chloride.
  - Physical state: Dark green crystals with bronze luster or crystalline powder with melting point of 190°C
  - Solubility: Soluble in water; sparingly soluble in alcohol and chloroform, solutions in water and in alcohol are deep blue in color
  - Packaging and storage: is kept in a tightly closed container, stored at room temperature in a dry area.

- **Polymers**
  - Poly(R-3-hydroxybutyrate) (PHB, 250 kDa, Nantian Co. Ltd., Jiangsu, China)
  - Polyethylene glycol 4000 (PEG 4000) (Fluka AG, Buchs SG, Switzerland)

- **Other materials**
  - Span 80 (Guang dong Guanghua chemical factory Co. Ltd., China)
  - Chloroform (Sigma-Aldrich, UK)
  - Ethanol Absolute (Sigma-Aldrich, Germany)
  - Sodium chloride (Adwic, El-Nasr Pharmaceutical Co., Abuzaabal, Egypt)
  - Potassium dihydrogen orthophosphate and sodium hydrogen phosphate dibasic (WINLAB, Leicestershire, UK)

- **Culture Media**
  Nutrient agar and nutrient broth (Oxoid Ltd; Basingostok; Hampshire, England)

- **Microorganisms**
  Methicillin resistant *Staphylococcus aureus* (MRSA) clinical isolate and a standard strain of *Staphylococcus aureus* ATCC 6538P (Sa_{st}) were obtained from the Department of Pharmaceutical Microbiology, Faculty of Pharmacy, Alexandria University.

2.2. Equipment

- Electrospinning apparatus equipped with High Voltage DC Power Supply (P3508, Raymax, Canada) and a syringe pump (101, KD scientific, USA)
- UV-Visible Spectrophotometer (T80 UV/ Vis PG Instruments Spectrophotometer. Ltd, England).
- Fourier Transform-Infra Red spectrometer (Perkin Elmer instruments, USA).
- Differential Scanning Calorimeter (DSC-6, CT, Perkin Elmer instruments, USA).
- Scanning Electron Microscope (JSM-5300, JEOL, Japan).
- Ion sputtering coater (JFC-1100E, JEOL, Japan).
- Adventurer sensitive electrical digital balance (Ohause Corp. Pine Brook, NJ, USA).
- pH-meter (pH 211, Hanna,).
- Vortex mixer (VM-300, KK ,USA)
- Hot plate magnetic stirrer (IP 21, IKA, Staufen, Germany)
- Digital camera, 12 mega pixels, 5X optical zoom (ES70, Samsung Co, South Korea).
- Thermostatically controlled shaking water bath (1083, GFL, Germany).
- Incubator (BST 5020, MLW, Germany)
- Portable autoclaves (A. Gallenkamp & Co. Ltd, United Kingdom).
- Micropipettes (Comecta, Spain).

2.3. Methods

2.3.1. Preparation of nanofibers (NFs) using emulsion electrospinning

Polyhydroxybutyrate (PHB)-based NFs were prepared using the emulsion electrospinning technique [69].

2.3.1.1. The electrospinning apparatus set-up

The electrospinning set-up (Figure 7) used for conducting electrospinning was assembled in-house. It consisted of a high voltage power supply to create a driving electrical force and digitally controlled precise syringe pump to control the flow rate of the liquid to be electrospun. A syringe with a blunt-tip stainless steel needle, with internal diameter of 0.5 mm was used. A positive high voltage was applied at the tip of a syringe needle (spinneret). The electrospun NFs were collected on an aluminum foil-covered metal plate (10 x 10 cm) connected to the negative high voltage. The spinneret was horizontally aligned with the collector plate. All preparations were performed at ambient temperature of ~ 25°C and relative humidity of < 65 %.

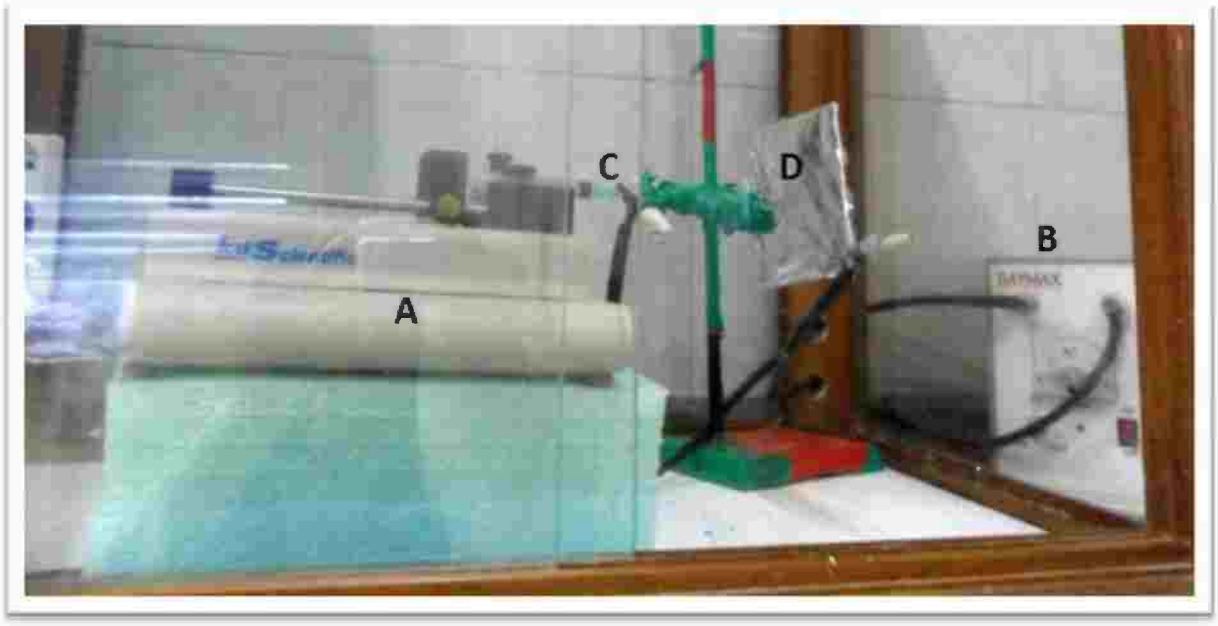

Figure 7: The electrospinning apparatus used in the study with its 4 main parts: A) syringe pump, B) high voltage generator, C) syringe with spinneret and D) aluminum collector plate.

2.3.1.2. Emulsion electrospinning for the preparation of MB-loaded PHB NFs

MB-loaded PHB-based NFs (PHB and PHB/PEG blend NFs) were prepared by emulsion electrospinning. The code numbers of NFs formulations and the formulation and processing parameters used for their preparation are shown in Tables 3 and 4.

A w/o emulsion was prepared using Span 80 as emulsifier. The organic phase was a PHB solution in chloroform. This was prepared by dissolving PHB in chloroform at 50 °C in screw-capped vials and then cooled to room temperature. Span 80 was added to make up the organic phase. Emulsions for electrospinning were prepared by dropwise addition of a specified volume of MB aqueous solution into the organic phase. The mixtures were stirred vigorously by vortexing for 10 min to obtain uniform emulsions. For the preparation of plain NFs, the aqueous phase consisted of distilled water. For formulations involving PHB-PEG blend, PEG was dissolved in the polymer solution.

The effect of different variables on the structural characteristics and pharmaceutical attributes of NFs was studied. These included: the concentrations of the polymer(s), Span 80 and MB as active agent in addition to the aqueous phase/ organic phase volume ratio.

The prepared emulsion was filled into the syringe which was then placed in the syringe pump and the needle connected to the high voltage. The flow rate, distance between the needle tip and the collector and the voltage were adjusted to obtain fine structured NFs. The applied voltage was

set in the range 10-22 kV. The distance between the needle and the collector was controlled (10-15 cm) to produce electric field strengths of 1 and 1.5 kV/cm. The polymer flow rate was adjusted to 1 ml/h. The electrospinning processes were performed in an air-conditioned laboratory at ambient temperature of 25°C and relative humidity of < 65 %. The fabricated NFs mat was removed from the collector, stored at ambient temperature in a desiccator to remove residual chloroform and water. NFs were kept away from light till characterization.

Table 3: Different formulations of MB-loaded PHB NFs

Ten NFs formulations were prepared by emulsion electrospinning using PHB as polymer at a constant flow rate of 1 ml/h.

<table>
<tr><th>Formula code</th><th>PHB (% w/v)</th><th>Aqueous phase/ organic phase ratio (v/v)</th><th>MB solution (% w/v)</th><th>Span 80 (% w/v)</th><th>Voltage (kV)</th><th>Distance (cm)</th></tr>
<tr><td>F_1</td><td>10</td><td rowspan="3">1:20</td><td>1.0</td><td rowspan="8">1</td><td rowspan="3">10</td><td rowspan="3">10</td></tr>
<tr><td>F_2</td><td>12</td><td>1.2</td></tr>
<tr><td>F_3</td><td>15</td><td>1.5</td></tr>
<tr><td>F_4</td><td rowspan="6">12</td><td rowspan="3">1.2</td><td>15</td><td>15</td></tr>
<tr><td>F_5</td><td>15</td><td>10</td></tr>
<tr><td>F_6</td><td>22</td><td>15</td></tr>
<tr><td>F_7</td><td>1:10</td><td>0.6</td><td rowspan="3">10</td><td rowspan="3">10</td></tr>
<tr><td>F_8</td><td>1:50</td><td>3.0</td></tr>
<tr><td>F_9</td><td rowspan="2">1:20</td><td rowspan="2">1.2</td><td>2</td></tr>
<tr><td>F_{10}</td><td>4</td></tr>
</table>

Table 4: Different formulations of MB-loaded PHB/PEG NFs

Nine NFs formulations were prepared by emulsion electrospinning using PHB/PEG blend, a constant Span 80 concentration (1% w/v of the organic phase), an aqueous phase/organic phase volume ratio of 1: 20, a voltage of 10 kV, a spinneret to collector distance of 10 cm and a flow rate of 1 ml/h.

Formula code	Polymer (% w/v)	Polymer composition	MB (% w/v)
F_{11}	12	PHB/PEG 4000 (95/5)	1.2
F_{12}		PHB/PEG 4000 (90/10)	
F_{13}		PHB/PEG 4000 (85/15)	
F_{14}		PHB/PEG 4000 (80/20)	
F_{15}		PHB/PEG 4000 (70/30)	
F_{16}		PHB/PEG 4000 (60/40)	
F_{17}	15	PHB/PEG 4000 (60/40)	1.5
F_{18}			2
F_{19}			3

2.3.2. Characterization of the prepared nanofibers

2.3.2.1. NFs morphology and diameter

The morphology of the NFs was investigated by scanning electron microscopy (SEM) with an accelerating voltage of 25 kV. The samples were coated with gold using an ion sputtering coater and examined by SEM at 2 magnification powers X 2000 and X 7500. The fiber diameter was measured from the SEM images of the samples using Digimizer 4© image software analyzer. Diameters of at least 50 random NFs were measured. The average fiber diameter was calculated and diameter distribution curves were constructed.

2.3.2.2. Fourier transform-infrared spectroscopy (FT-IR)

Samples of MB, PHB, PEG 4000, electrospun NFs meshes of PHB-PEG 4000, MB-PHB, MB-PEG, and their respective physical mixtures, in amounts equivalent to the ratios present in the NFs, were mixed in a mortar with KBr and compressed into discs. The samples were scanned from 500 to 4000 cm^{-1} using FT-IR system.

2.3.2.3. Thermal analysis

Differential scanning calorimetery (DSC) was performed on PHB, PEG and MB as well as plain and MB-loaded PHB-PEG (3:2) NFs. Samples, 5mg each, of the NFs and their respective physical mixtures, in amounts equivalent to the ratios present in the fibers, were weighed accurately. Indium standard was used to calibrate the DSC temperature and enthalpy scale. Samples were hermetically sealed in an aluminum pan. An empty pan was used as reference. Thermograms were obtained by heating at a constant rate of 5 °C/min, over a temperature range of 25-400°C. Inert atmosphere was maintained by purging nitrogen at a flow rate of 20 ml/min.

2.3.2.4. Determination of MB content and encapsulation efficiency (EE)

The MB content of loaded NFs was determined using an extraction procedure. Briefly, an accurately weighed amount (20 mg) of the loaded NFs was placed in 5 ml absolute ethanol in well-closed screw capped vials and sonicated. The extracted MB was determined by UV spectrophotometric analysis at λmax 654 nm, and the process was repeated till complete extraction of MB which was confirmed spectrophotometrically and by complete bleaching of NFs. MB concentration for each ethanolic solution was calculated using a pre-constructed calibration curve for MB in absolute ethanol and the total MB loading was calculated. Results are the mean of three determinations for samples from different batches. The actual MB load was calculated as the mg MB/g of polymer and the encapsulation efficiency was calculated using the following equation:

$$\text{Encapsulation efficiency \%} = \frac{\text{Actual MB content}}{\text{Theoretical MB content}} \text{ x } 100$$

2.3.2.5. *In vitro* drug release studies

The release of MB was determined in PBS pH 7.4 at 37°C under sink conditions. Electrospun MB-loaded nanofibrous mats were sectioned into squared pieces containing 0.4 mg of MB (as detected by EE) and placed separately in 20 ml of the release medium in 50 ml capped Erlenmeyer flasks. The flasks were shaken in a thermostatically controlled shaking water bath at 30 stroke / min. At pre-determined time intervals, 2 ml-sample of the release medium was withdrawn and replaced with the same volume of fresh medium pre-equilibrated to 37°C. The concentration of released MB was determined spectrophotometrically at λmax 660 nm using a pre-constructed calibration curve in PBS. All release experiments were run in triplicate and the mean values of percentage drug released were calculated after correction for sample replacement.

To test for possible re-uptake of released MB by NFs, adsorption of MB to plain NFs under simulated release conditions was investigated. Plain NFs samples were immersed separately in 20 ml PBS pH 7.4 containing a MB amount equivalent to the actual load of MB-loaded NFs. Samples were shaken in a thermostatically controlled shaking water bath at 37° C at 30 stroke / min. At scheduled time intervals, 2 ml-sample of the medium was withdrawn and replaced with the same volume of fresh PBS pre-equilibrated to 37°C. The concentration of MB remaining in the medium was measured spectrophotometrically at λmax 660.

A modified release study was also undertaken using the same regular release procedure above but the release medium was completely replaced with fresh medium at all sampling times.

2.3.2.6. Water uptake assessment

Water uptake by MB-loaded PHB and PHB-PEG (3:2) NFs prepared using a 15% w/v total polymer solution was assessed by gravimetric analysis before and after incubation in PBS. A NFs sheet was sectioned into squared pieces weighing ≈ 60 mg. Samples were allowed to dry in a desiccator for one week. Weights of dry samples (W_1) were determined prior to immersion in the buffer using an analytical balance. Samples were then immersed in 20 ml PBS (pH 7.4) and incubated at 37 °C. The samples were removed at pre-determined time points over a period of 24 h. The swollen fiber meshes were gently blotted with filter paper to remove excess surface water and their wet weight was recorded (W_2). After weighting, they were returned to PBS to test for further water uptake. All experiments were run in triplicate and water uptake was calculated using the following formula.

$$\% \text{ Water uptake} = \frac{W2 - W1}{W1} x\ 100$$

2.3.2.7. *In vitro* degradation of the NFs:

The degradation of test MB-loaded PHB and PHB-PEG (3:2) NFs prepared using a 15% w/v total polymer solution was studied at 37°C using PBS pH 7.4 as degradation medium. Individual NF samples, squared NFs pieces weighing ≈ 15 mg, were separately submerged in 5 ml PBS in sealed tubes which were placed in an incubator maintained at 37ºC without agitation. Samples were removed at different time intervals over 60 days. Removed samples were rinsed with distilled water and dried in vacuum till constant weight. The mass loss was calculated from the percentage weight remaining using the following equation:

$$\% \text{ Weight remaining} = \frac{W2}{W1} x\ 100$$

W_1 and W_2 were the initial weight and the weight remaining after incubation. All experiments were run in triplicate.

2.3.2.8. Antimicrobial activity of MB solution and MB-loaded NFs

2.3.2.8.1. Test microorganisms and bacterial culture

The two bacterial strains under study, namely standard *Staphylococcus aureus* ATCC 6538P (Sa_{st}) and MRSA1 clinical isolate were maintained at 4°C as slant cultures of sterile nutrient agar for a maximum of one month [272]. The purity of each strain was always checked by streaking on nutrient agar plate and microscopical examination. Long term preservation was performed by freezing in 15% glycerol broth [273].

For each microorganism, one loopful from its stock slant culture was streaked onto the surface of nutrient agar plate and incubated at 37°C for 18-24 h for isolation. Several resulting morphologically similar colonies were subcultured into 3 ml nutrient broth, and incubated at 37°C for 18-24 h. The inoculum was used after 2 successive broth subcultures. The CFU/ml of the final inoculum was adjusted by proper dilution with sterile saline to obtain an inoculum size of about 10^8 CFU/ml.

Culture media were prepared according to the manufacturer's directions. In case of liquid media, they were distributed in appropriate containers (test tubes and flasks) and plugged before sterilization. The media were sterilized, unless otherwise stated, by autoclaving at 121ºC for 15 min. After cooling to 50ºC, the sterilized media were distributed as required in sterile Petri dishes and tubes and were left to solidify. The plates and tubes of culture media were then incubated at 37ºC overnight before use to ensure absence of microbial contamination.

2.3.2.8.2. Antibacterial activity of MB solution against the two test organisms

The antibacterial activity of MB solution was assessed against the two test organisms (Sa_{st} and MRSA) using the microdilution method [274] over a MB concentration range of 0.488 to 125 µg/ml. The MB stock solution (0.25 mg/ml) was serially diluted two-fold with sterile saline in 96-well microtitre plates. Aliquots of 100 µl overnight broth subcultures of the test microorganism were diluted with double strength nutrient broth to reach a final inoculum of about 10^6 CFU/ml and added to 100 µl of MB solution in each well. Samples were incubated in the dark for 24 h at 37°C. The % transmittance was measured for samples at 450 nm using a microplate reader. Inoculated and non-inoculated wells containing 200 µl antimicrobial-free nutrient broth were included side by side with the wells containing MB. Further investigation was done using the plate surface counting technique of the surviving organisms after incubation for 24 h verified the purity of the culture from any microbial contamination. Aliquots (100 µl) of samples were serially diluted ten-fold with sterile saline. Aliquots of 20 µl of each dilution were dropped using sterile disposable tips fitted to a calibrated micropipette onto the surface of over-dried nutrient agar plates. The plates were incubated at 37ºC for 24 h, the resulting colonies were counted and the number of survivors was determined using the following equation:

Number of CFU/ml = (Average count/drop) x 50 x dilution factor

All Experiments were performed in duplicate.

2.3.8.2.3. Antibacterial activity of MB-loaded NFs using the agar diffusion method

The effect of emulsion electrospinning process on the antibacterial activity of the encapsulated MB was tested against MRSA using the agar diffusion technique [275]. Circular samples weighing 5 mg of PHB-PEG (3:2) NFs loaded by encapsulation (5mg/g) were tested for their antibacterial activity against MB solution (0.25 and 0.5 mg/ml). Equal volumes of both solutions (50 µl) were dropped using a calibrated micropipette into 7 mm-diameter wells preformed in agar plates using sterilized cork borer. The plates were inoculated using adjusted inocula (10^6 CFU/ml) that gave semi-confluent growth of colonies after overnight incubation. Inoculation was done by swabbing in three directions for even spreading over the entire plate surface. The activity of the released MB was compared to MB solutions after 24 h incubation at 37°C by measuring the diameters of inhibition zones in millimeters. Experiments were performed in duplicate.

2.3.8.2.4. MB release from MB-loaded NFs in bacterial culture

The release of MB from PHB-PEG (3:2) NFs loaded by encapsulation (5mg/g) was carried out in presence of MRSA. Circular samples of 1 cm diameter and weighing =12 mg were sectioned out of the prepared sheet. MB content of three samples was measured by extraction with ethanol as previously described. In 24-well plate, each NFs sample was immersed in the release medium consisting of 200 µl bacterial suspension and 200 µl sterile saline giving a final bacterial count of ~10^6 CFU/ml (as confirmed by viable count technique). The samples were incubated at 37°C with shaking at 75 stroke / min for different time intervals (0.25, 0.5, 1, 2, 4, 6, 24 h) in the dark. At each time interval, 200 µl-aliquots of the release media of 3 samples were

removed by pipetting. Samples were diluted to 1 ml with sterile saline and sonicated for 15 minutes to lyse the bacteria that had partially taken-up the released dye [276]. Samples were centrifuged at 4000 x g for 10 minutes to precipitate the bacterial cells debris. The concentration of MB in the aspirated supernatant was calculated by spectrophotometric analysis at 660 nm. All samples were kept in the dark and experiments were carried out in triplicate.

2.3.2.8.5. Antibacterial activity of MB-loaded NFs using the viable count technique

The antibacterial effect of PHB-PEG (3:2) NFs on the growth of the two test bacterial strains (Sa_{st} and MRSA) after 24 h exposure was determined using the viable count technique. Circular samples of PHB-PEG (3:2) NFs with 1 cm diameter and weighing ≈ 12 mg were used. Samples were placed inside separate wells of 24-well plates. Aliquots (200 µl) of the broth culture of the test organism suspension (~10^6 CFU/ml) were added to each well. Aliquots of 200 µl of sterile nutrient broth were added. Samples were incubated in the dark at 37° C. The experiment was carried out in two groups: one group of which aliquots were withdrawn for bacterial counting after 1 h while the other group was sampled at 24 h. Control groups were prepared by adding 200 µl inoculum to 200 µl nutrient broth (positive control). All experiments were carried out in triplicate and the results were expressed as mean survival bacterial count (CFU/ml) and % mean surviving bacteria from the maximal viability counts determined from control bacterial cultures that were not exposed to MB as in the following equation:

$$\text{Percentage surviving bacteria} = (N/N_0) \text{ X } 100$$

Where N_0 is the number of CFU / ml from control bacterial cultures not exposed to MB and N is the number of CFU/ ml in the samples treated.

2.3.3. Statistical analysis

The generated data were subjected to statistical analysis using a one way analysis of variance test followed by a post Newman-Keuls test with $P \leq 0.05$ denoting significance. Analysis was done using GraphPad Prism 5 © software.

3. Results and discussion

A general objective of the work in this thesis was to develop MB-functionalized electrospun nanofibers for effective exploitation of the structural characteristics and multifunctionality of nanofibrous matrices coupled with the various biological effects of MB. Specific objectives were to assess the *in vitro* and *in vivo* performance of these matrices in selected local biomedical applications.

In this chapter of the thesis, MB-eluting nanofibers matrices were prepared using essentially polyhydroxybutyrate (PHB) as polymer matrix. Because of MB hydrophilicity, emulsion electrospinning was used as a modified electrospinning technique used for fabrication of NFs incorporating water soluble drugs [59, 60, 62, 63]. Formulations and processing parameters were modulated to determine conditions leading to the production of NFs with target pharmaceutical attributes, drug release pattern in particular, as a major factor contributing to in-use performance.

3.1.MB-loaded PHB NFs

3.1.1. Formation and morphological characteristics of PHB NFs

3.1.1.1. Effect of polymer concentration

In the process of polymer electrospinning, stable continuous fibrous mats can be obtained only above a critical polymer concentration depending on its Mw and below a process limiting viscosity [277]. The effect of PHB concentration (10, 12 and 15% w/v) in the organic phase on NFs formation was investigated while other parameters were kept constant. PHB polymer grade used in this study (Mw 250 kDa) failed to form defect-free NFs at a 10% w/v concentration level. Intense bead formation was observed (Figure 8). Increasing PHB concentration to 12 or 15 % enabled the formation of non-beaded NFs with average fiber diameter (AFD) of 490 ± 58 and 675 ± 129 nm respectively (Figure 8 and Table 5). Bead formation at low polymer concentration has been previously linked to low viscosity of the electrospun jet [238]. Under such conditions, the surface tension has a greater influence than the too low viscoelastic forces and likely leads to a breakup of the electrospun jet with the formation of beads and/or beaded nanofibers [278]. The significant increase in AFD at 15% PHB as compared to 12% PHB NFs ($p < 0.001$) can be attributed to increased resistance to the elongation of the electrospun jet as a result of increased emulsion viscosity at higher PHB concentration [279]. The narrowest size distribution was observed at 12% PHB (Figure 8).

High encapsulation efficiency exceeding 95% was observed at both 12 and 15 % PHB concentrations (Table 5) indicating suitability of the emulsion electrospinning process adopted for encapsulation of hydrophilic charged molecules such as MB into PHB. Further investigation of the effect of different process and formulation parameters on the 12 % PHB NFs was therefore carried out.

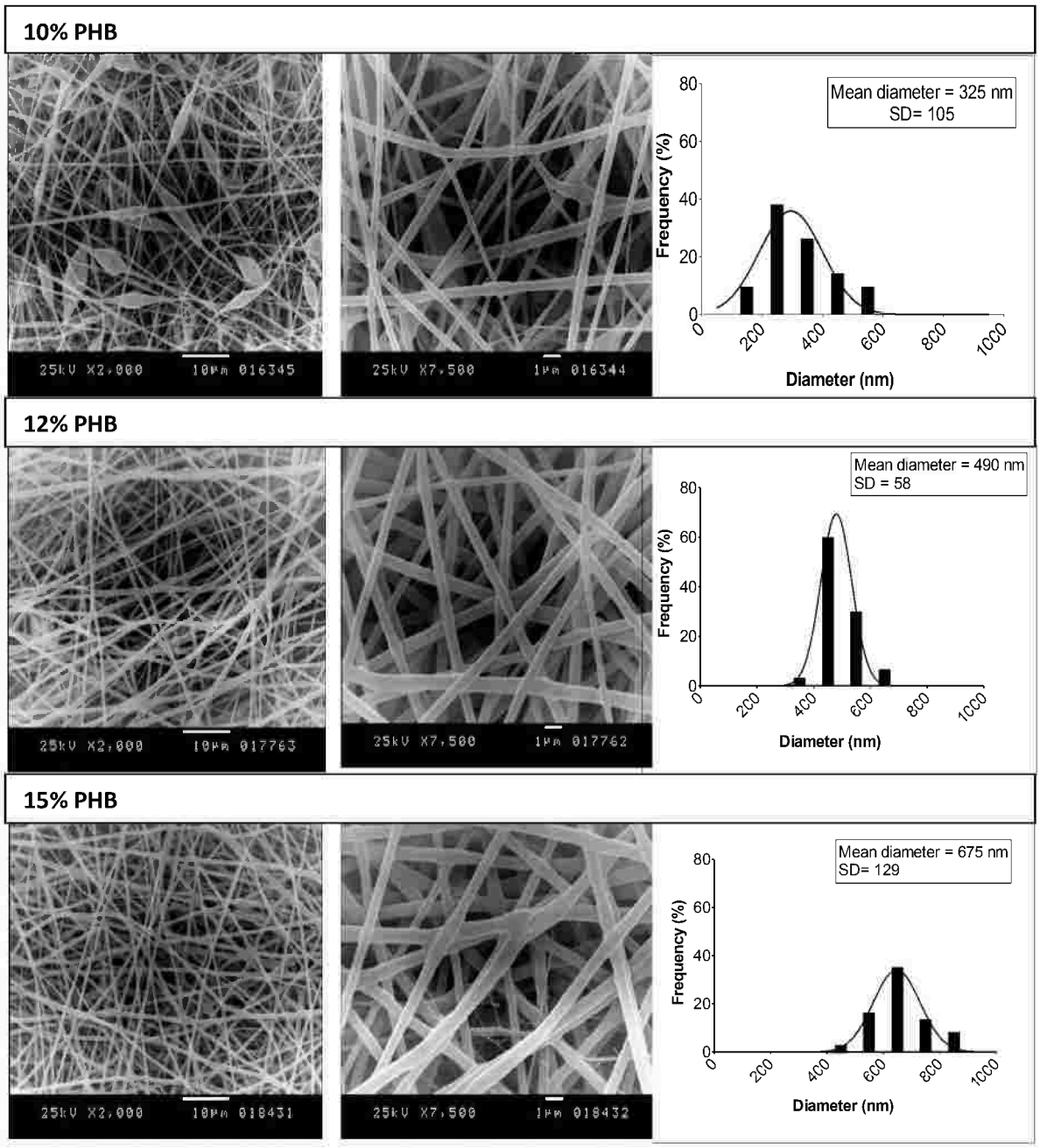

Figure 8: Scanning electron micrographs and fiber diameter distribution curves of MB-loaded PHB NFs with different PHB concentrations: 10, 12 and 15 % w/v, at 2 magnification powers 1: X 2000 and 2: X 7500

* Experimental variables: 10kV/10 cm, Span 80 1% w/v, aqueous: organic phase ratio 1:20 and MB content 5 mg/g of polymer weight.

Table 5: Effect of polymer concentration on the diameter of PHB NFs and MB encapsulation efficiency (EE %)

Polymer concentration (% w/v) [a]	Average fiber diameter (AFD) (nm) ± SD	EE% ± SD
10	325 ± 105	N.D.
12	490 ± 58	95.5 ± 2.94
15	675 ± 129	99.1 ± 2.52

[a]Aqueous: organic phase volume ratio: 1:20, MB loading: 5mg/g, Span 80: 1% w/v
[b] N.D.: not determined

3.1.1.2. Adjustment of the electrospinning processing parameters: Voltage and tip to collector distance

In the electrospinning process, the electric field (EF) is defined as the applied voltage divided by the working distance between the needle tip and the collector. MB-loaded 12% PHB NFs were electrospun under the effect of two electric field strengths (1 and 1.5 kV/cm) by varying both the voltage (10, 15 and 22 kV) and the tip to collector distance (10 and 15 cm) as shown in Figure 9. Increasing the EF strength by increasing the voltage at constant working distance resulted in an insignificant decrease in the AFD ($p > 0.05$). However, a broader distribution of fiber diameters was observed, probably due to the larger numbers of very thin filament-like fibers formed. During electrospinning, the voltage applied to the polymer solution induces high charge accumulation at the needle tip. Hence, excess charge on the surface of the fluid jet is driven by the field toward the counter electrode pulling the solution and initiating a Taylor cone, followed by jet formation [23]. By increasing the EF strength, the jet surface has a greater excess of charge, leading to a relatively smaller decrease in surface charge density and field strength over the travelled distance. Additionally, increasing the EF strength increases the electrostatic repulsive force in the fluid jet which ultimately favors potentiated jet stretching, leading to decreased fiber diameter. It is worth noting that keeping the strength of applied EF constant by concomitant change of the voltage and working distance did not affect AFD significantly ($p > 0.05$). A narrower size distribution of the NFs was also observed at lower EF of 1 kV/cm. Therefore, electrospinning parameters were set to 10 kV/10 cm in subsequent experiments.

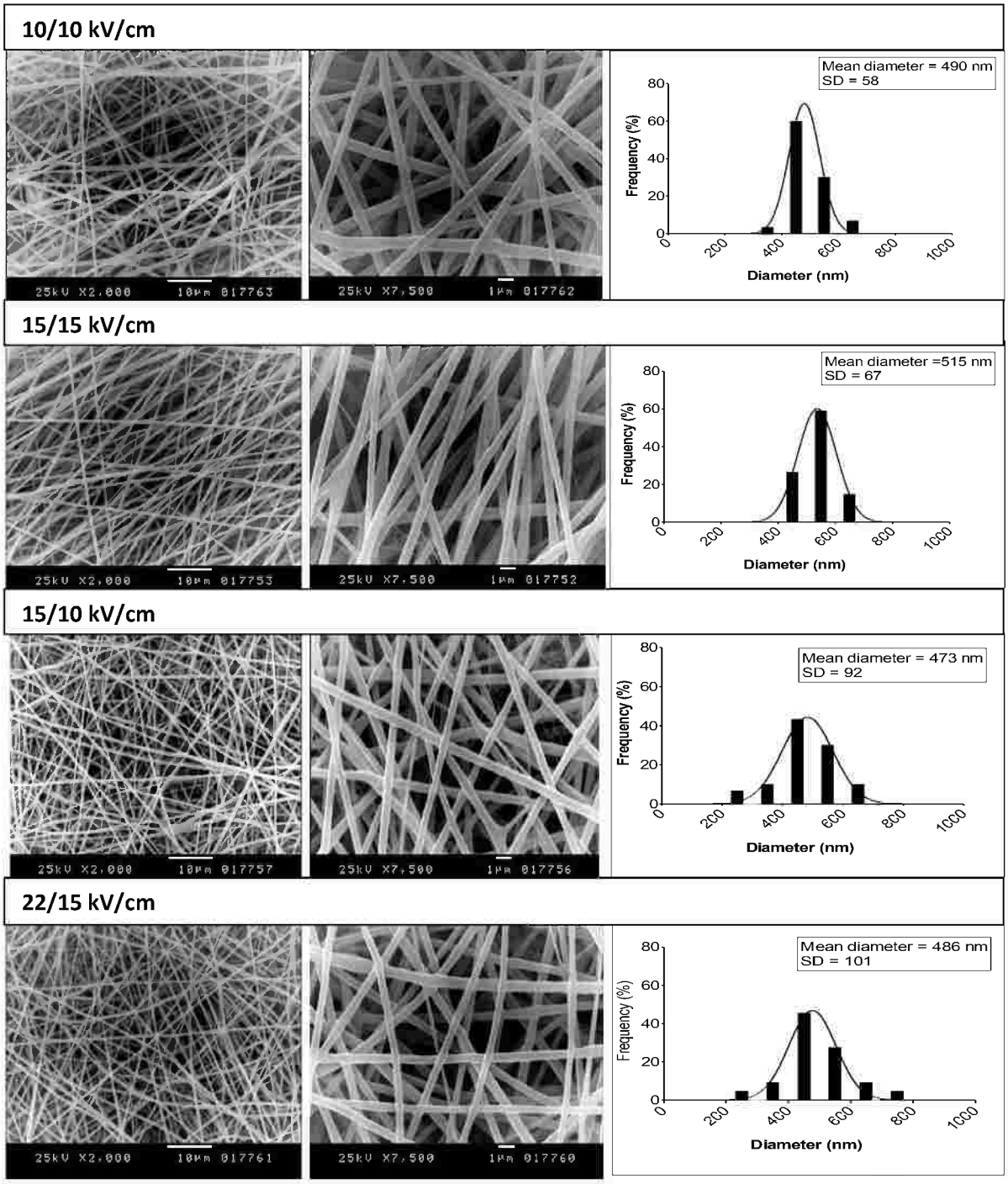

Figure 9: Scanning electron micrographs and fiber diameter distribution curves of MB-loaded PHB NFs electrospun under the effect of different voltage and working distance: 10/10, 15/15, 15/10 and 22/15 kV/cm, with 2 magnification power 1: X 2000 and 2: X 7500

* Formulation parameters; 12%w/v PHB, Span 80 1% w/v, aqueous: organic phase ratio (1:20) and MB content 5 mg/g of polymer weight

3.1.2. Modulation of MB release characteristics

MB-loaded NFs with release patterns suitable for biomedical applications may call for slow long term elution of the antimicrobial agent or a biphasic release profile allowing relatively fast early availability of MB followed by slower progressive elution. These include mainly prophylactic applications such as the prevention of surface colonization of implanted membranes or devices [203] and relatively short term antimicrobial applications such as the healing of infected wounds respectively [257].

MB release from PHB NFs was modulated by controlling two emulsion formulation variables, the phase volume ratio and the emulsifier concentration.

3.1.2.1. Effect of the phase volume ratio on MB encapsulation and release

NFs prepared from electrospun emulsions with an aqueous: organic volume ratio of 1: 10 showed significantly lower encapsulation efficiency as compared to those prepared using lower aqueous factions, 1: 20 and 1: 50 (Table 6). Emulsion stability is a crucial factor for enhancing EE. No signs of instability were observed for any of the test emulsions throughout the electrospinning process. However, microscopic droplet instability/ segregation may account for the reduced EE at the 1: 10 phase volume ratio [280]. MB EE exceeded 90% at both 1: 20 and 1: 50 ratios with no significant difference between the 2 formulations ($p > 0.05$).

Release profiles of MB from the three test emulsion formulations are shown in Figure 10. Biphasic release profiles characteristic of matrix structure were obtained. An initial MB burst was followed by a slower release phase for five days reaching a plateau which extended over 30 days. The relatively faster initial release rate could be attributed to diffusion of the drug near the fiber surface. A fraction of MB may allocate near the surface due to its partial solubility in chloroform. Charged MB molecules would also move to the outer region of the electrospinning jet in effect of charge repulsion [53, 281]. The slow and incomplete release phase may be attributed to the high crystallinity of PHB, which could limit the diffusion of the aqueous environment into the nanofibrous matrix, limiting the diffusion of the drug from the fibers [11] and slow degradation of PHB

Table 6: Effect of aqueous: organic phase volume ration on MB encapsulation and burst release from PHB NFs

Phase volume ratio	Encapsulation efficiency % ± S.D.	1 hr burst release %
1:10	85.35 ± 9	31
1:20	95.45 ± 2.9	27
1:50	92.48 ± 6.9	21

[a] Polymer concentration: 12% w/v, MB loading: 5mg/g, Span 80 concentration: 1%

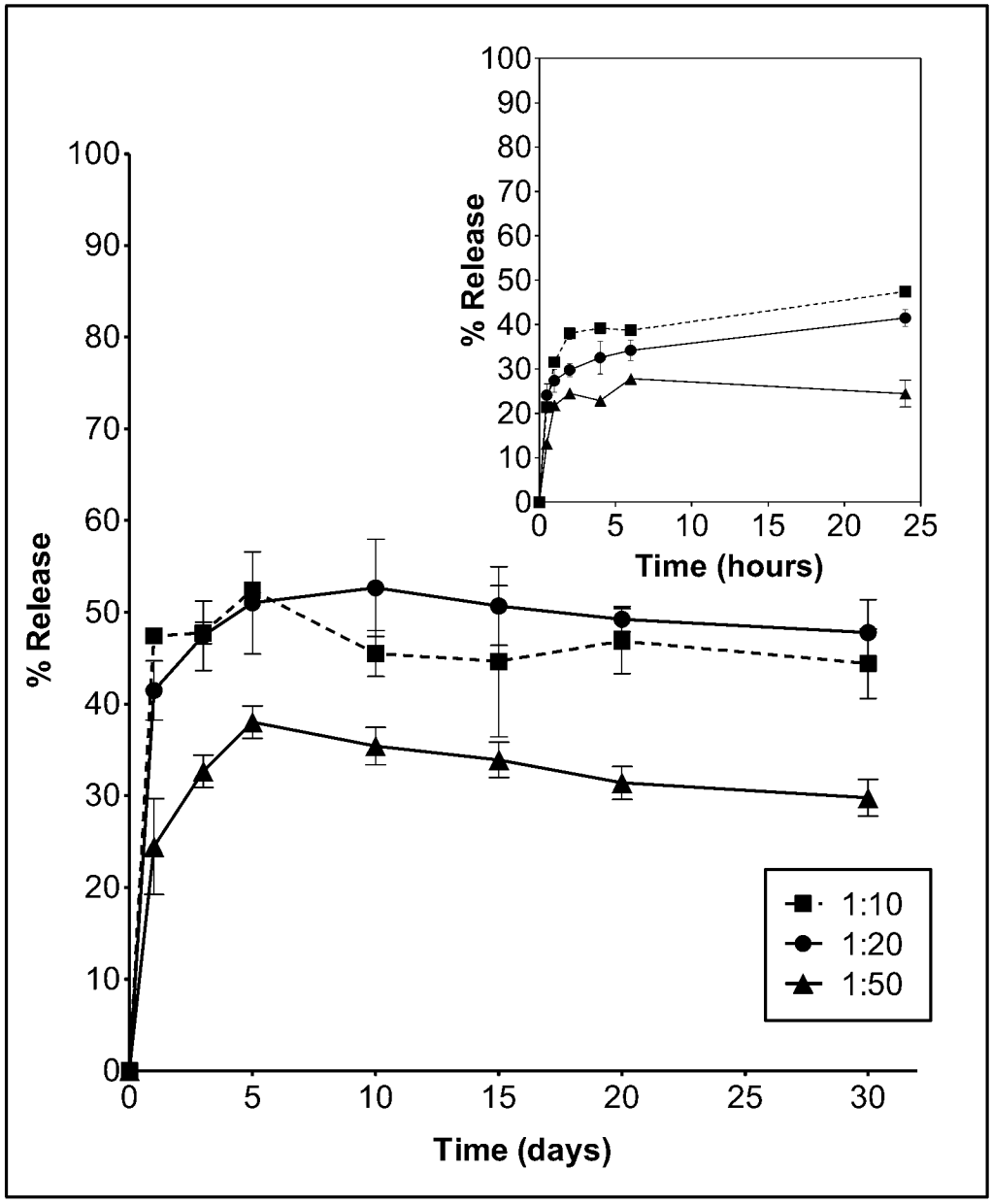

Figure 10: Effect of the aqueous: organic phase volume ratio of emulsion on MB release from MB-loaded NFs prepared with 12% PHB, in PBS pH 7.4 at 37°C for 30 days. Inserted figure highlights release profile over the first 24 h

Figure 10 shows that a phase volume ratio of 1: 10 of the emulsion used for PHB NFs electrospinning resulted in the highest 1h initial burst of MB, 31% in comparison to 27 and 21 % respectively. Differences were significant ($p<0.05$) only between burst release data for NFs prepared using 1: 10 and 1: 50 phase volume ratios. At 6 h, the % released of MB from NFs prepared with 1: 10 and 1: 20 ratios was significantly higher ($p<0.05$ and <0.01 respectively) compared to those prepared with the 1: 50 ratio. Thereafter, and over 5 days, release rates for both 1: 10 and 1: 20 ratios were comparable and higher than the rate observed for the 1: 50 ratio (Figure 10). Results indicated that initial MB release can be effectively modulated by increasing the aqueous volume fraction. A larger aqueous phase fraction in emulsion electrospinning was reported to increase the porosity of NFs [280]. The hydrophilic moiety on the core would tend to move outward simultaneously with fiber solidification, and larger and more numerous channels would form throughout the fiber matrix [61]. In addition, water has relatively low volatility, and larger fractions may not be able to completely evaporate during electrospinning leading to rapid phase segregation and encapsulation of larger water droplet within the solidifying polymer phase. The trace amount of water left-over in the nanofibrous mats could enable the movement of the polymer chains and further enhance the migration of MB molecules nearby the NFs surface [237]. Taken together, a phase volume ratio of 1: 20 was considered suitable for further electrospinning experiments.

3.1.2.2.Effect of the emulsifier concentration on MB encapsulation and release

The effect of Span 80 used as emulsifier on the EE% and MB release from emulsion electrospun NFs was investigated in the concentration range 1 to 4% w/v. NFs prepared using emulsions stabilized with 1% w/v Span 80 showed an EE of 95.5% (Table 7). Increasing the emulsifier concentration to 2% w/v had no significant effect on the EE. However, a further increase to 4% w/v resulted in a significant decrease in the EE ($p<0.05$). As previously noted, such reduction is mainly indicative of emulsion destabilization. It has been previously shown that a surfactant concentration window exists, out of which the emulsion stability quickly declines [282]. At low emulsifier concentration, the emulsion is unstable because of agglomeration of the oil droplets. At high emulsifier concentration emulsion instability occurs because of rapid coalescence. Accordingly, Span 80 was used at a concentration level of 1% w/v of the oil phase in subsequent experiments.

Table 7: Effect of Span 80 concentration on MB encapsulation and burst release from PHB NFs

Surfactant concentration (%w/v)	Encapsulation efficiency % ± S.D.	1 h burst release %
1	95. 5 ± 2.9	27
2	96.9 ± 3.1	17
4	82.9 ± 3.1	9

* PHB concentration: 12% w/v, MB loading: 5mg/g and aqueous: organic phase ratio: 1:20

Apart from its effect on MB EE, an increase in Span 80 concentration was associated with a lower initial release rate during the first 6 h (Figure 11). At 0.5, 1 and 2 h time points, NFs prepared with 1% Span 80 released significantly higher ($p<0.01$) amounts of MB than those prepared with 2 and 4% emulsifier. Data for burst release at 1 h are shown in Table 7. However, comparable release profiles proceeded up to 30 days. It is well established that nonionic surfactants confer emulsion stabilization by film formation and steric stabilization at the water droplet interface, thus preventing flocculation [283]. The observed reduction of initial MB release rates in association with increased Span 80 concentration may be attributed to the facile migration of the excess non film forming emulsifier molecules to the NFs surface during rapid solvent evaporation. It was reported previously that Span 80 on PLGA NFs surface could prevented the prompt penetration/diffusion of water molecules into the NFs, thus retarding drug release [281].

In general, MB release took place according to a biphasic profile (Figures 10 and 11) including a relatively large initial burst followed by an extended slower release phase. This pattern may be actually needed in antimicrobial applications for early elimination of the intruding bacteria before they begin to proliferate and inhibition of population of the organisms that may survive the initial burst [30]. Release data obtained indicated that a change of the aqueous: organic phase volume ratio and emulsifier concentration of the emulsion used for NFs electrospinning could, to a certain extent, modulate MB release, particularly the early release phase. However, in all cases, the % MB release did not exceed 54% approximately, implying possible contribution of MB-PHB interactions to the observation and restricting possible applicability to long term infection-prevention antimicrobial applications.

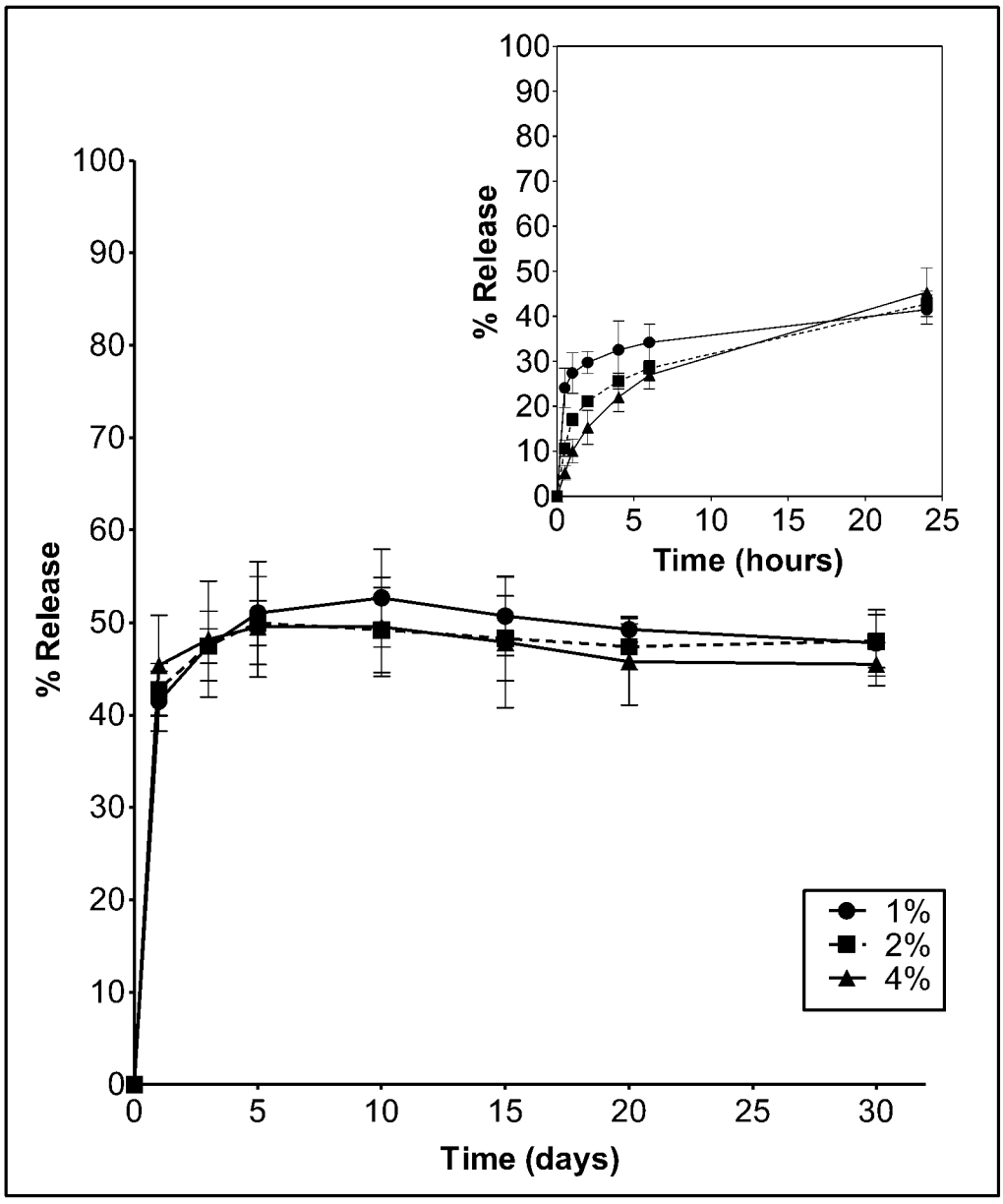

Figure 11: Effect of Span 80 concentration on MB release from MB-loaded 12% PHB NFs in PBS pH 7.4 at 37°C for 30 days. Inset: MB release data for 24 h

3.1.3. Fourier transform-infrared spectroscopy

FTIR spectra of MB, PHB and their electrospun and physical mixtures are presented in Figure 12. MB spectrum showed a very strong sharp absorption band at 1591 cm-1 corresponding to vibrations of the aromatic ring. The C–H 'in plane' vibrations were found between 1240 and 1034 cm^{-1} and 'out of plane' vibrations were at 947 and 662 cm^{-1}. The peak corresponding to the C-H stretching vibration was found at 2922 cm^{-1}. A characteristic very strong absorption band appearing at 1321 cm^{-1} is due to the C–N stretching vibration. For PHB, a characteristic sharp strong absorption band appeared at 1724 cm^{-1} corresponding to carbonyl (C=O) stretching vibrations. The stretching of hydroxyl (O–H) groups appeared as small sharp peak at 3436 cm^{-1}. The other characteristic bands for PHB were observed at 1280, 1183, and 1057 cm-1, which can be assigned to the vibration of the ester (C-O-C) groups of the polymer. The bands centered at 979, 1228, 1280, and 1724 cm^{-1} were shown to arise from the crystalline phase of PHB.

To elucidate the types of interactions between MB and PHB, a binary mixture of MB and PHB was electrospun and its spectrum was compared with that of the corresponding physical mixture. The FT-IR spectrum of the physical mixture was a superimposition of the spectra of individual components. For electrospun MB-PHB mixture, reduction of peak intensity, shifts and broadening of peaks were observed when compared to the spectrum of the physical mixture and the spectra of individual MB and PHB. The peak at 1323 cm^{-1} corresponding to C–N stretching in MB has diminished. Vibrations of the aromatic ring at 1590 cm^{-1} have also diminished. Broadening of the peak at 3436 cm^{-1}, corresponding to O-H stretching in PHB was observed. Furthermore, the intensity of the C=O stretching was highly reduced. Thus, it became clear that the peaks corresponding to –CN group in MB, –OH group and C=O in PHB were affected. It can be concluded that the –OH group of the polymer interacts with the nitrogen atom (C-N) on the MB with hydrogen bonding. In addition, there is an ionic interaction between the positively charged quaternary amine (N^+) of MB and the negatively charged carbonyl (COO^-) group of PHB.

3.1.4. Thermal analysis

The thermal properties of electrospun PHB-based NFs were examined using DSC to investigate possible drug-polymer interactions as well as the effect of the formulation process on PHB physical properties and thermal stability [284]. Thermograms of PHB, MB, plain and MB-loaded electrospun mats and their corresponding physical mixtures are shown in Figure 13. PHB thermogram showed two endothermic peaks at 174 and 276 °C corresponding to PHB melting and decomposition temperatures respectively, which is in agreement with literature data [285]. MB thermogram exhibited a small exothermic peak at 214 °C, corresponding to thermal decomposition reported to take place in conjunction with its melting.

To investigate the effect of electrospinning on PHB thermal properties, plain electrospun PHB was examined by DSC. As compared to the thermogram of PHB, shifts of the melting and decomposition peaks to 170 and 258 °C, as well as the appearance of a shoulder right before the melting peak can be observed. This could be due to the improvement in the orientation of molecular chains within the electrospun polymer NFs, as well as the larger area to volume ratio of electrospun fibers [286, 287]. In addition, the crystallinity of the fiber structure is expected to decrease appreciably when compared to the unprocessed polymer. In other words, the chain entanglement in bulk form is much higher when compared to the same polymer in nanofibrous matrix [286].

Encapsulation of MB within PHB NFs resulted in disappearance of the MB melting exotherm at 214 °C. Due to the relatively low MB content in the sample, this observation was not conclusive regarding the physical state of MB within the NFs, whether molecularly dispersed or crystalline. On the other hand, shift of the melting peak to 170°C possibly indicated MB-PHB interaction. Finally, emulsion electrospinning led to efficient evaporation of the solvent and the internal aqueous phase as no extra peaks were observed below 100°C [239].

In conclusion, both FT-IR and DSC examinations revealed that MB interacts with PHB possibly by H-bonding and electrostatic interactions which, in conjunction with high degree of polymer crystallinity, may account for the earlier results of this study showing incomplete MB release from PHB NFs for up to a 30 day-study period.

A

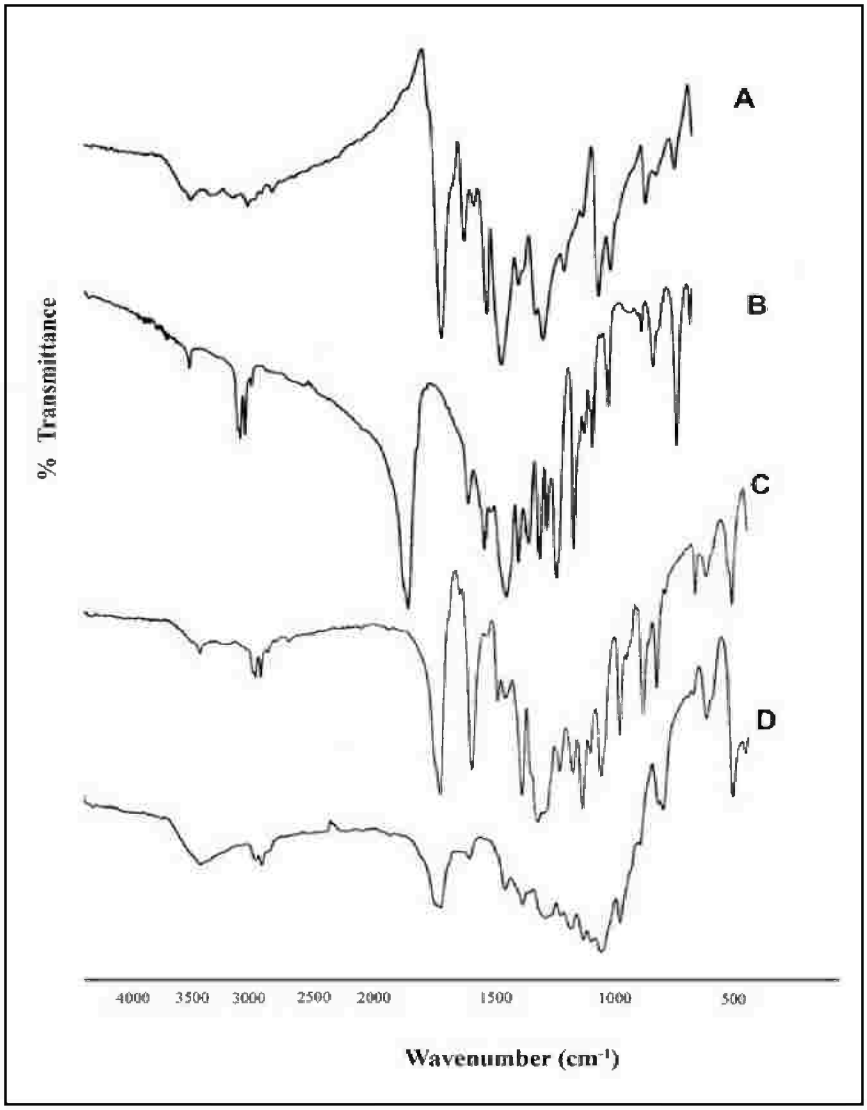

Figure 12: IR spectra of A) MB, B) PHB, C) MB-PHB (1:4) physical mixture, and D) electrospun MB-PHB (1:4)

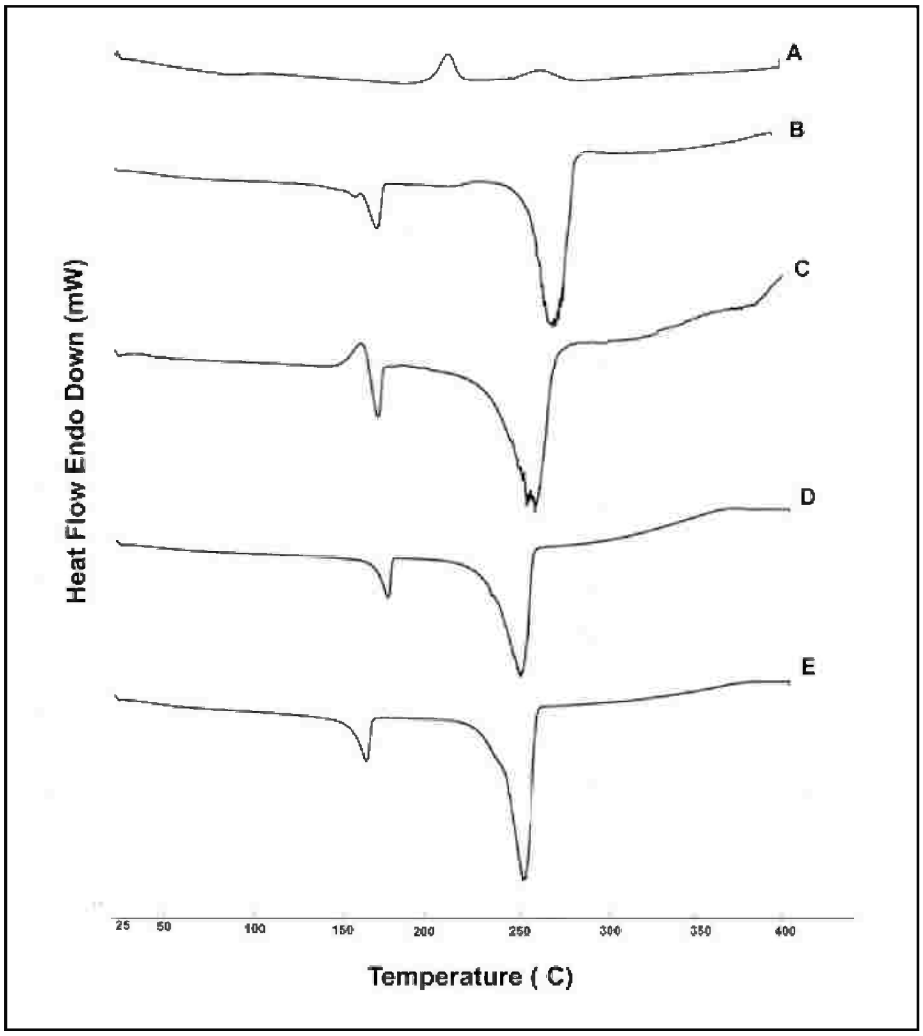

Figure 13: DSC thermograms of A) MB, B) PHB, C) Plain PHB NFs, D) MB-PHB physical mixture, and E) MB-loaded PHB NFs.

3.2.MB-loaded PHB/PEG blend NFs

Hydrophilization of the NFs polymer matrix, by facilitating penetration of the release medium into the matrix, may be a simple approach to enhance MB release. Polymer matrix hydrophilization can be achieved by copolymerization or blending with hydrophilic [224, 226]. In this study, PHB/PEG blends containing 5 to 40% w/w PEG of the total polymer content (PHB/PEG ratios: 9:1, 8: 2, 7: 3 and 6: 4) were electrospun using the formulation and process parameters adjusted for PHB NFs These were: polymer concentration: 12% w/v, Span 80: 1% v/v, aqueous: organic phase ratio: 1:20 and MB content: 5 mg/g of polymer weight. All formulations were electrospun at 10kV/10 cm

3.2.1. Formation and morphology of PHB-PEG blend NFs

Electrospinning of MB loaded PHB-PEG blends containing up to 30% PEG produced smooth defect-free NFs**.** AFDs of these polymer blend NFs were not significantly different from those prepared from PHB (Figure 14). However, increasing PEG weight ratio to 40% resulted in rather deformed NFs associated with the appearance of fused connections at the fiber crossing points. The observation may be attributed to fusion of PEG in PEG-rich spots formed during the electrospinning process [240]. Expectedly, morphological defects were associated with a significant ($p< 0.001$) increase of the AFD to 663 ± 140 nm as compared with other blend NFs with lower PEG content. This blend had also the widest fiber diameter distribution among tested formulations. Increasing PEG content to 50% of the total 12% w/v polymer concentration resulted in increasing the fibrous mat fragility producing easy to fragment mat. Hence, an attempt was made to obtain well-structured NFs by increasing the total polymer concentration to 15%.

Plain and MB-loaded PHB-PEG NFs were electrospun from emulsions prepared with 15% w/v of the polymer blend. These were compared with PHB NFs regarding morphological characteristics and NFs diameter (Figure 15). Results indicated that at the 15% polymer blend concentration, incorporation of 40% w/w PEG into the blend did not adversely affect the fiber morphology. Neither fusion points nor structural deformations were observed. This may be attributed to reduced polymer phase segregation during electrospinning as a result of the higher viscosity of the polymer organic solution. In terms of AFD, PHB-PEG (3:2) blend NFs had a significantly smaller AFD 611 ± 168 nm ($p< 0.001$) compared to plain PHB NFs (AFD 913 ± 197 nm), probably due to enhanced stretching of the lower viscosity polymer blend solution during electrospinning. MB loading caused a further reduction of AFD to 411 ± 103 nm, with largely reduced fiber diameter distribution range (Figure 15). These effects are likely due to increased electrical conductivity of the spun emulsion and charge density of the polymer jet leading to easier elongation of the polymer jet [19]. A similar finding was reported for PEG–PLA NFs loaded with tetracycline hydrochloride [234]. It is noteworthy that the AFD of MB-loaded PHB/PEG blend 3: 2 (411 nm) was also significantly ($P < 0.001$) smaller than that of PHB NFs (675 nm) with similar MB loading (Figure 8).

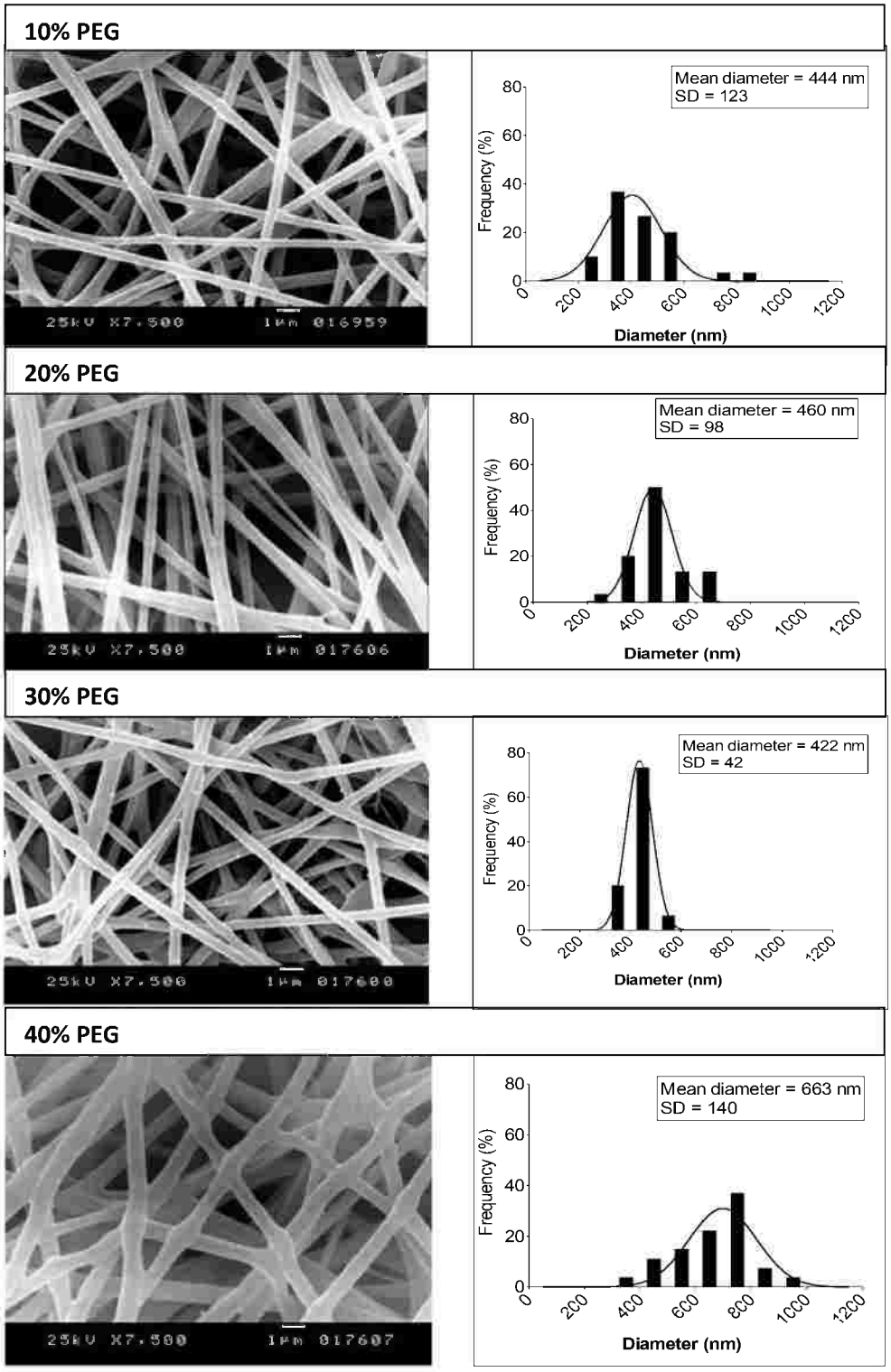

Figure 14: Scanning electron micrographs and fiber diameter distribution curves of MB-loaded PHB/PEG blend NFs prepared with total polymer concentration of 12%w/v and different PEG 4000 content: 10, 20, 30 and 40%.

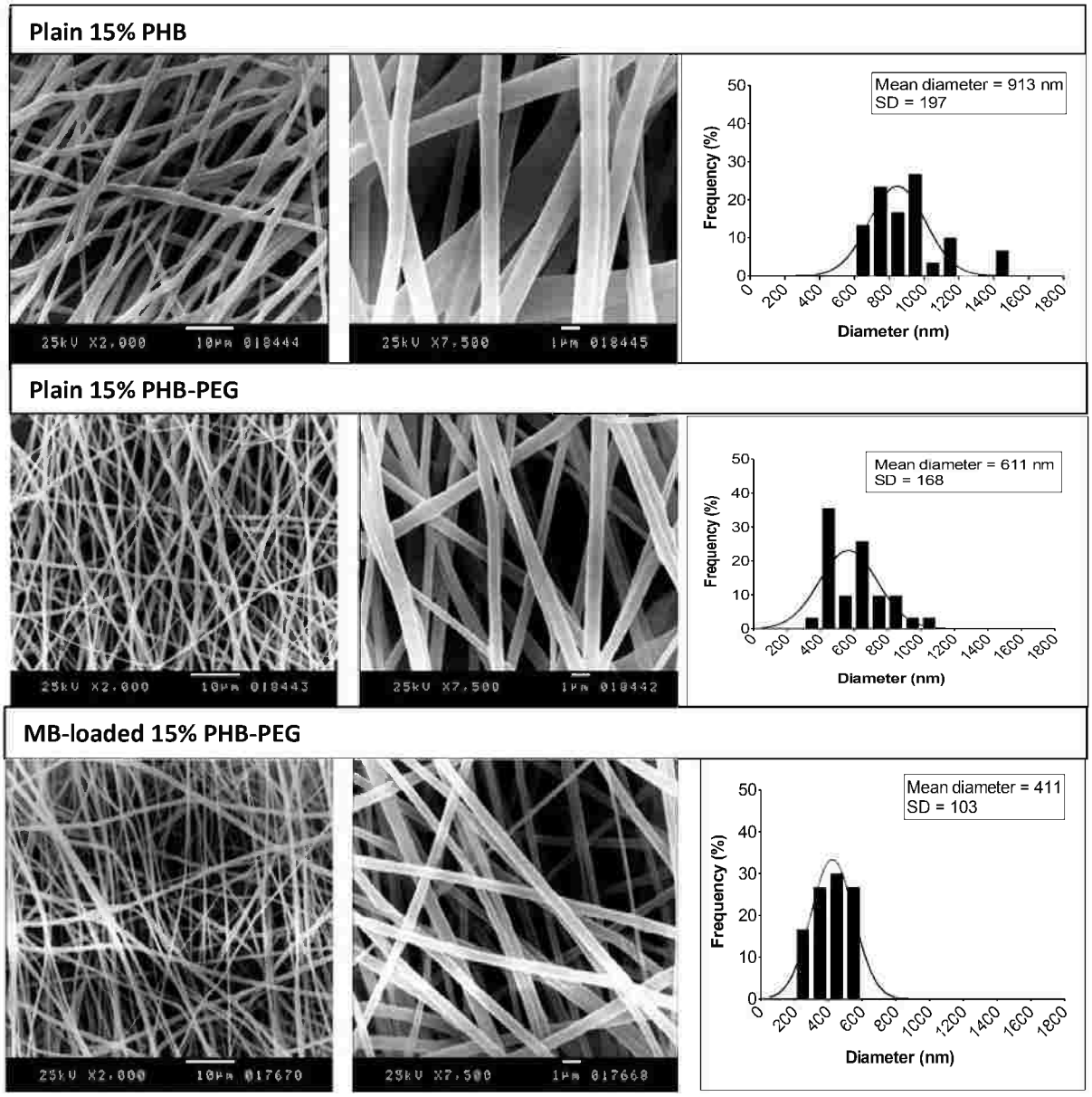

Figure 15: Scanning electron micrographs and fiber diameter distribution curves of plain PHB NFs, plain PHB/PEG (3:2) blend NFs and MB-loaded PHB/PEG (3:2) blend NFs, prepared using 15% w/v total polymer solution.

3.2.2. Entrapment efficiency and MB loading

The effect of selected formulation variables on MB EE% and MB load (mg/g) into PHB-PEG blend NFs was studied. These included: % PEG in the polymer blend (5-40%), polymer solution concentration and MB theoretical load in selected formulae.

Results indicated that at 12% w/v total polymer solution concentration and theoretical MB loading level of 5mg/g, blending PHB with up to 40% PEG 4000 did not result in a significant ($p>0.05$) change in MB EE%, with all formulation attaining EE higher than 92%. At 15% w/v total polymer solution concentration, increasing the MB load of PHB/PEG blend (3:2) NFs resulted in reduced EE%. Starting with a theoretical load of 6.6 mg/g resulted in a reduction of EE% to 80.33 ± 6.8, however, this did not translate to lower MB load as compared to that obtained from 5mg/g theoretical load. Using 10 mg/g theoretical load, and despite the reduction of EE% to 73.3 %, significantly ($p<0.001$) increased the MB load to 7.33 ± 1.27 mg/g. However, this was accompanied by observed instability in the fabricated NFs visualized as dark violet coloured spots in the fibrous mat. Stretching-induced de-emulsification during emulsion electrospinning has likely yielded highly conductive phase at the highest MB load tested. Such solution/phase was observed to be extremely unstable in the presence of strong electric fields, which led to a dramatic bending instability [288].

3.2.3. Fourier transform-infrared spectroscopy

To investigate possible interactions between NFs formulation components, FTIR spectra of MB, PHB, PEG, their electrospun and physical mixtures were recorded (Figure 16). Analysis of MB and PHB spectra were previously discussed under section *3.1.3.* PEG spectrum showed absorption bands at 1282, 1242 and 1109 cm^{-1} corresponding to the vibration of the C-O-C groups and another characteristic band at 3436 cm^{-1} corresponding to OH-stretching.

For electrospun PHB/PEG, the peak at 1724 cm^{-1} corresponding to C=O stretching in PHB was shifted to 1729 cm^{-1}. The peak at 3437 cm^{-1} corresponding to O-H stretching in PHB or PEG showed broadening and decrease in intensity when compared to the corresponding peaks of PHB and PEG respectively. While the peak at 1109 cm^{-1} referring to the C-O-C stretching in PEG decreased in intensity. Furthermore, a large decrease in intensity was observed for the peak at 2888 cm^{-1} due to C-H stretching in PEG. In this case, interaction could not be highly confirmed by FTIR as both PEG and PHB contain O-H and C-O-C groups. However, there is a possible interaction between PEG and PHB (H-bonding). In case of electrospun MB/PEG, the strong absorption band at 1590 cm^{-1} corresponding to the vibrations of aromatic ring has been diminished, otherwise the spectrum of electrospun MB/PEG superimposed that of the corresponding physical mixture, indicating no specific interactions between MB and PEG.

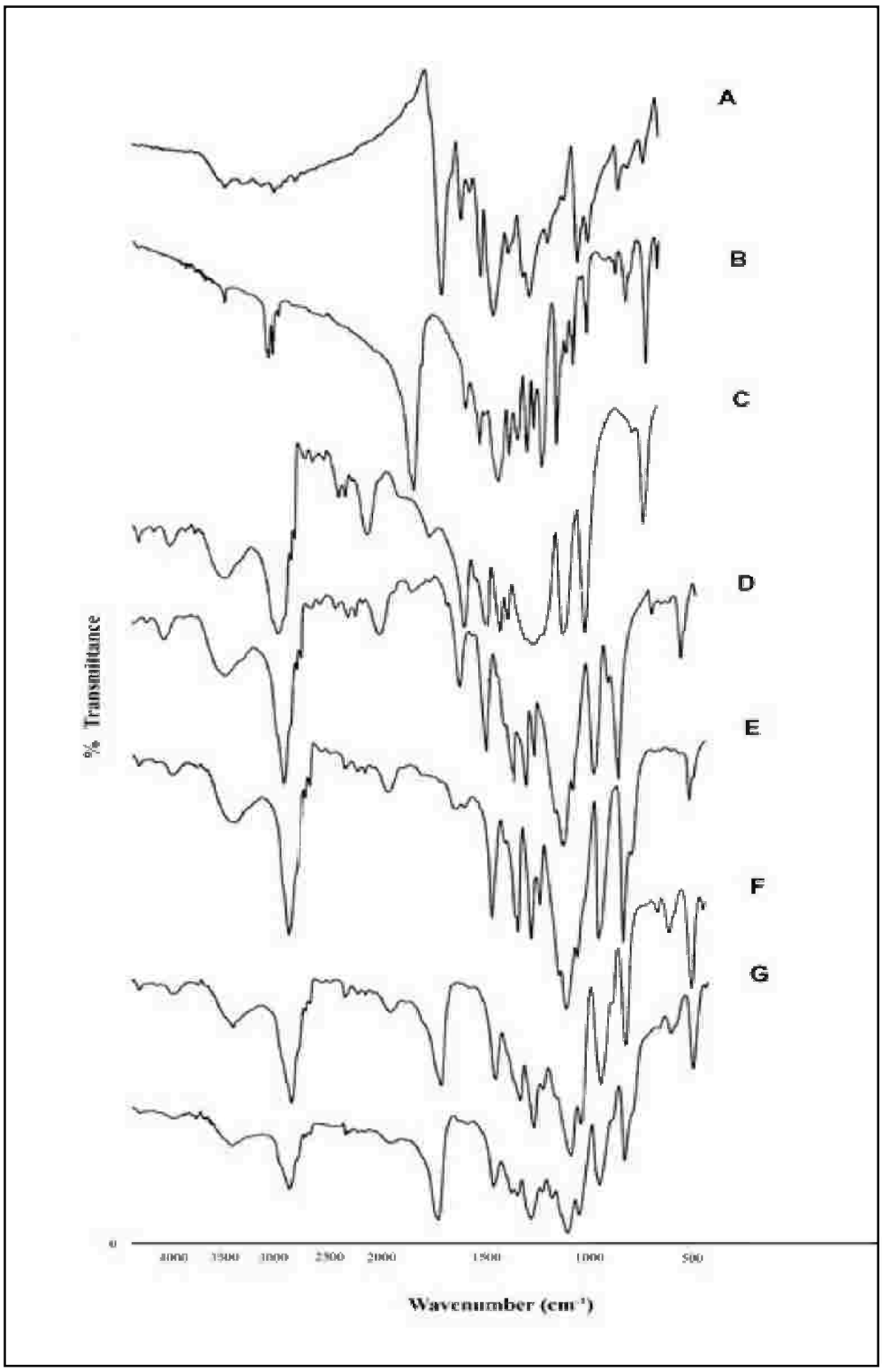

Figure 16: IR spectra of A) MB, B) PHB, C) PEG, D) MB-PEG (1:4) physical mixture, E) electrospun MB-PEG (1:4), F) PHB-PEG (4:1) physical mixture and G) electrospun PHB-PEG (4:1).

3.2.4. MB Release studies from PHB-PEG blend NFs

Release profiles from PHB-PEG blend NFs are shown in Figures 17 and 18. In general, enhanced MB release rates were obtained from various blend NFs, even those containing as low as 5% PEG, compared to those from non blended PHB NFs. Significantly higher 1h MB burst from NFs containing 15-40 % PEG was observed ($p<0.05$ for 15 and 20 % PEG, $p<0.001$ for 30 and 40 % PEG). These results would be mainly due to increased hydrophilicity and enhanced water uptake capacity of the blend nanofibrous matrices, predisposing PEG dissolution and formation of porous/channeled NFs matrix structure with further enhanced capillary water intake and MB leaching. The porogenic effect of PEG in polymeric matrix systems including NFs has been previously reported [72]. For PHB-PEG (3:2) blend NFs, increasing the polymer solution concentration from 12% to 15% w/v reduced initial MB release rate (Figure 19). This is probably due to the previously suggested less homogenous matrix structure of the blend NFs prepared at 12% total polymer concentration (Figure 14). In such a structure, MB would tend to preferentially accumulate in the hydrophilic PEG rich islets and get promptly released in conjunction with PEG dissolution.

On the other hand, consistent decline of the cumulative amount of MB released was observed for all PHB-PEG blend NFs tested. The time to decline points decreased as the PEG weight fraction increased; that is 10 days, 3 days, 4 h, and 6 h for NFs containing 5-15%, 20%, 30%, and 40% PEG respectively. Since sink conditions prevailed throughout the experiment, the observation pointed out that the release settings may not be merely controlled by simple diffusion kinetics but rather by diffusion-adsorption equilibrium kinetics. The assumption was further supported by the observed faster and extensive decline in case of blend NFs containing 40% PEG as compared to that seen with blend NFs containing 30% PEG. An observation that probably correlates to the increased surface porosity/area of the 40% PEG blend NFs and faster MB release at the peak point of its release profile (75 ± 6 %), both correlations are characteristic of adsorption controlled settings. In the second release phase up to 30 days, all release profiles apparently equilibrated and leveled off around 50% cumulative amount of MB released (Figure 18). Observed fluctuations of release profiles during this phase are likely due to transient equilibrium disturbance by medium dilution following each sampling point. It is noteworthy that MB photobleaching is not a contributing factor to the observed fluctuations since all experiments were light protected. MB as a cationic dye has been previously adsorbed to other polymeric NFs [289, 290]. In this study, MB adsorption to PHB-PEG (3:2) NFs was confirmed by running an adsorption experiment under simulative release study conditions, the results are shown in Figure 20.

Modification of the release study design was carried out to allow non-interrupted MB release. Release medium was, therefore, completely replaced with fresh medium at each sampling point. The modified conditions are more closely related to the *in vivo* situation where the released drug is continuously drained off the release site by natural clearance mechanisms. The modified procedure was tested using PHB-PEG (3:2) blend NFs prepared with 15% w/v polymer solution concentration. Under the modified release conditions, the cumulative amount of MB released at 24 h reached 83 ± 3 % and the release further proceeded over a week to 90% without declines or fluctuations (Figure 21).

It is important to note that, MB release from non blended PHB NFs prepared with 15% w/v polymer solution concentration, showed 39% MB released at 24 h with minor amounts of drug released up to 40 days and none over the next 20 days (Figure 22). The release pattern is rather similar to that obtained previously under non modified release conditions, confirming that earlier incomplete MB release patterns from PHB NFs were, as previously interpreted, mainly dominated by polymer matrix properties and drug-polymer interactions rather than interrupted by MB resorption.

In conclusion, MB-loaded PHB-PEG (3:2) NFs were selected for further investigation since this formulation combined good morphological characteristics, high MB loading efficiency and high initial release rate with almost complete release within a week; a profile suitable for short term antimicrobial applications such as wound healing.

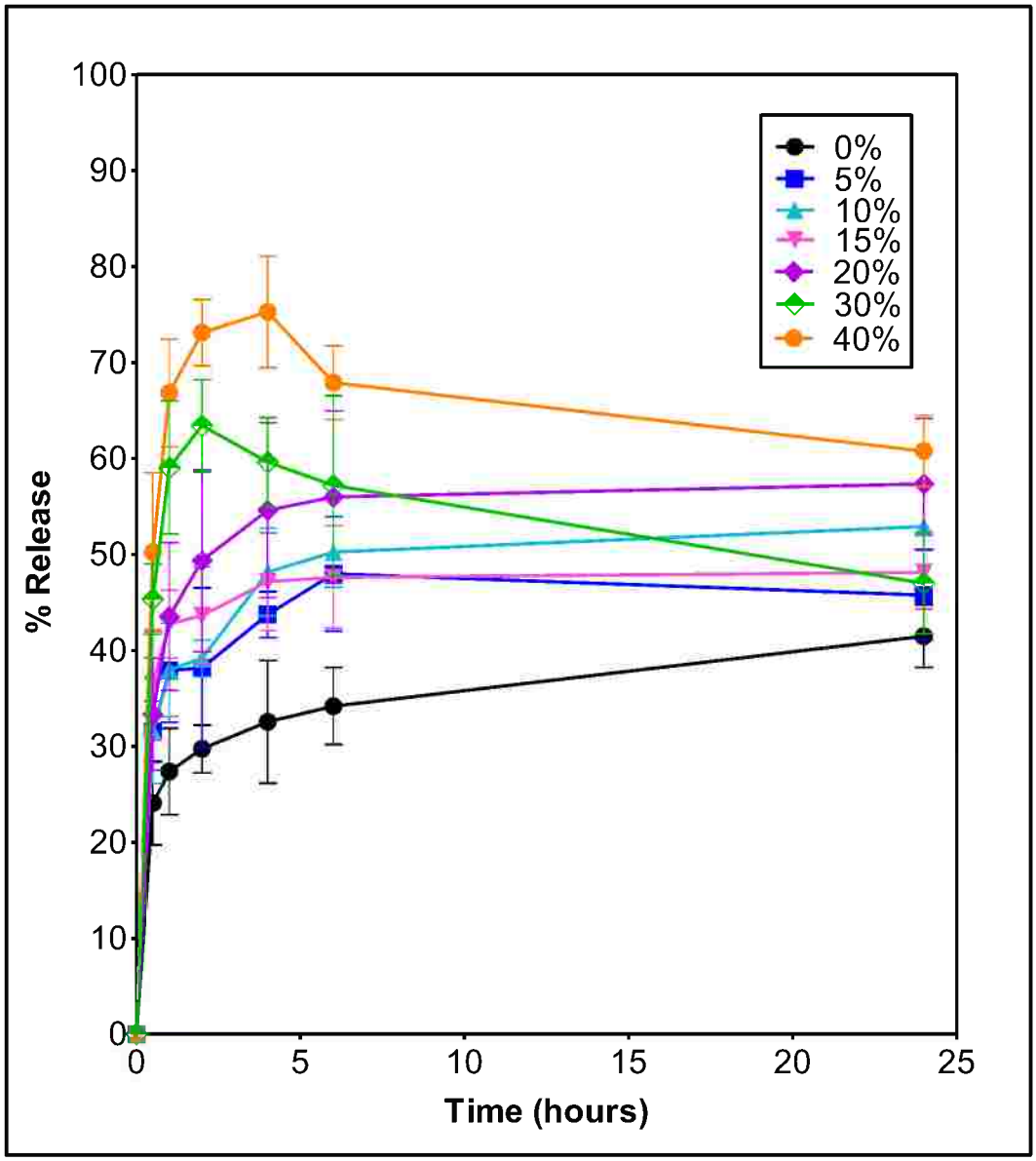

Figure 17: Effect of PEG 4000 content on MB release from MB-loaded NFs for 24 h in PBS pH 7.4 at 37°C (polymer solution concentration 12%w/v)

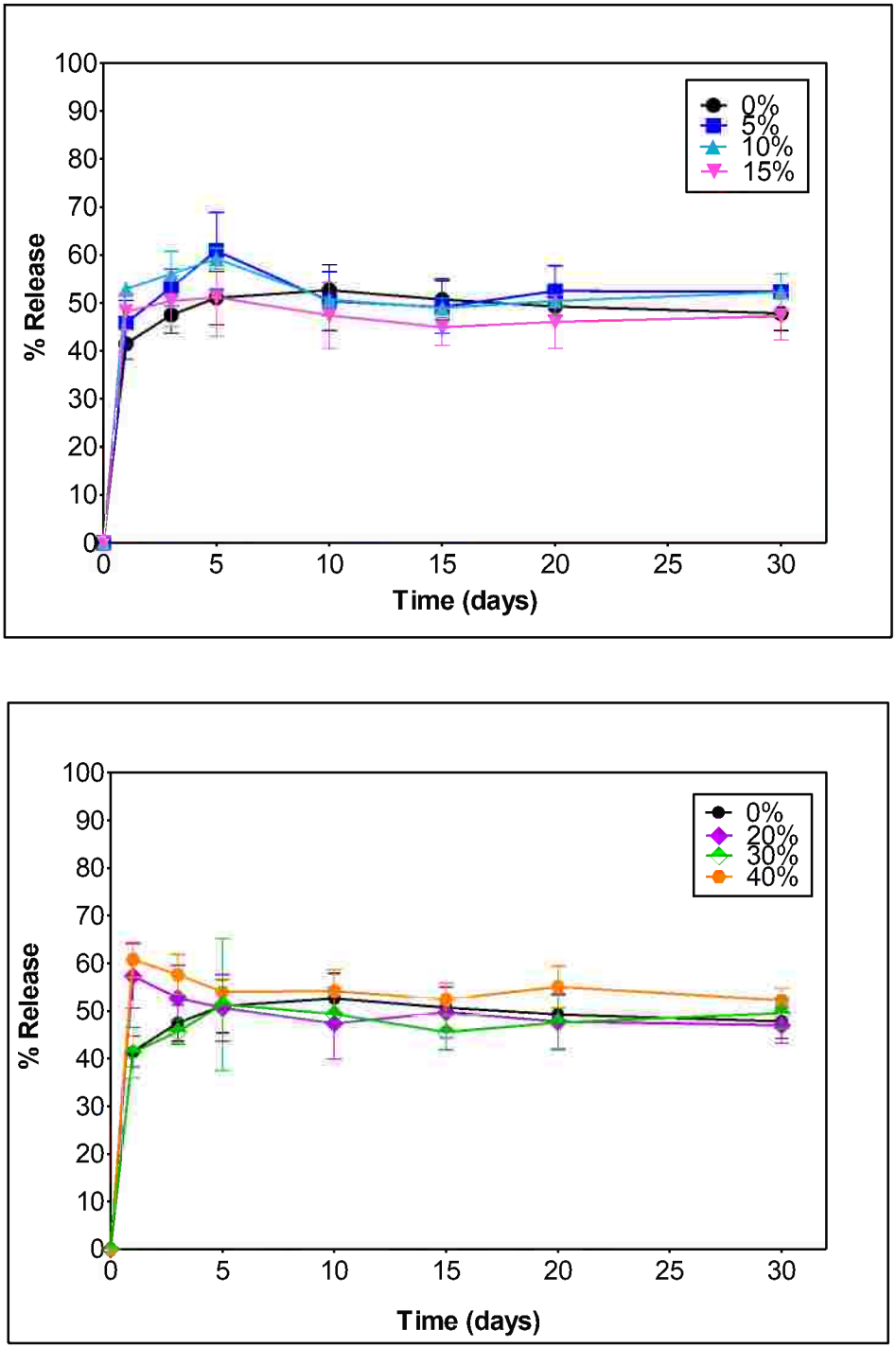

Figure 18: Effect of PEG 4000 content on MB release from MB-loaded NFs for 30 days in PBS pH 7.4 at 37°C (polymer solution concentration 12%w/v)

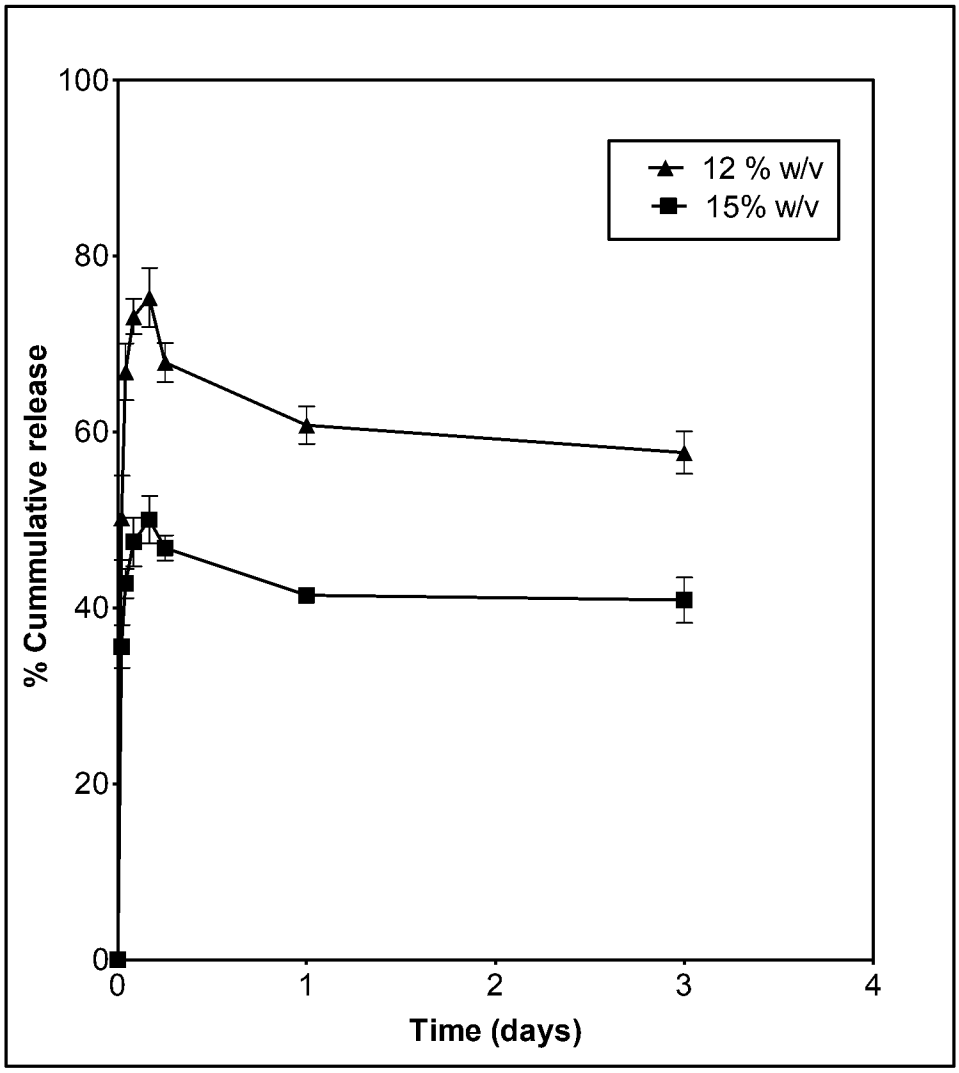

Figure 19: Effect of polymer solution concentration on MB release from MB-loaded PHB/PEG (3:2) NFs in PBS pH 7.4 at 37°C.

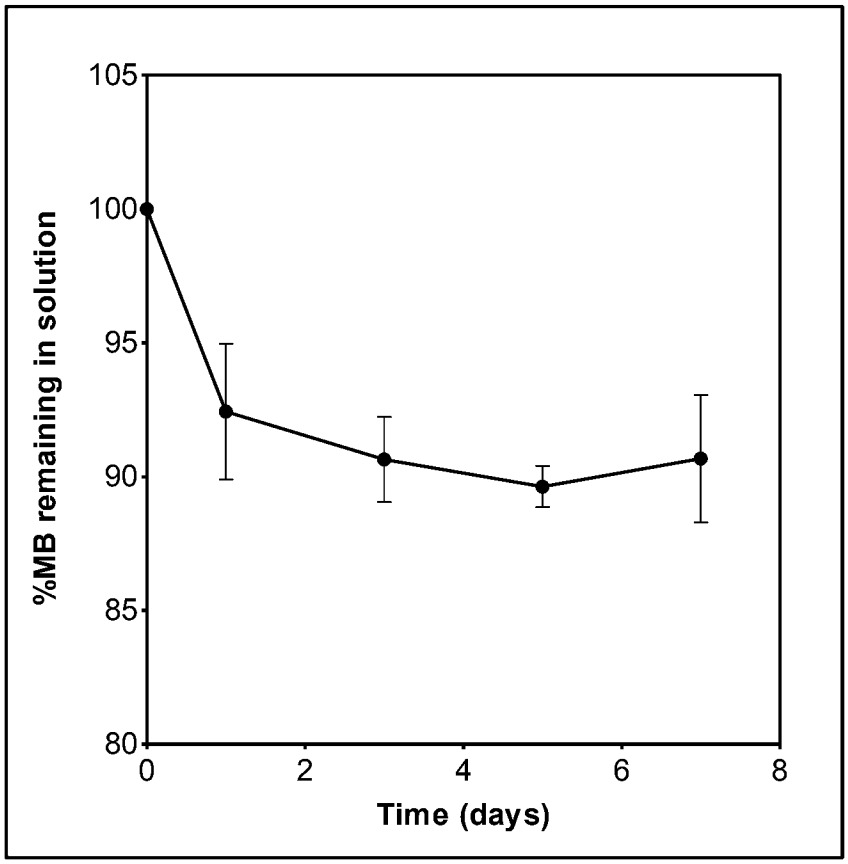

Figure 20: MB adsorption by plain PHB/PEG (3:2) NFs under simulated release conditions

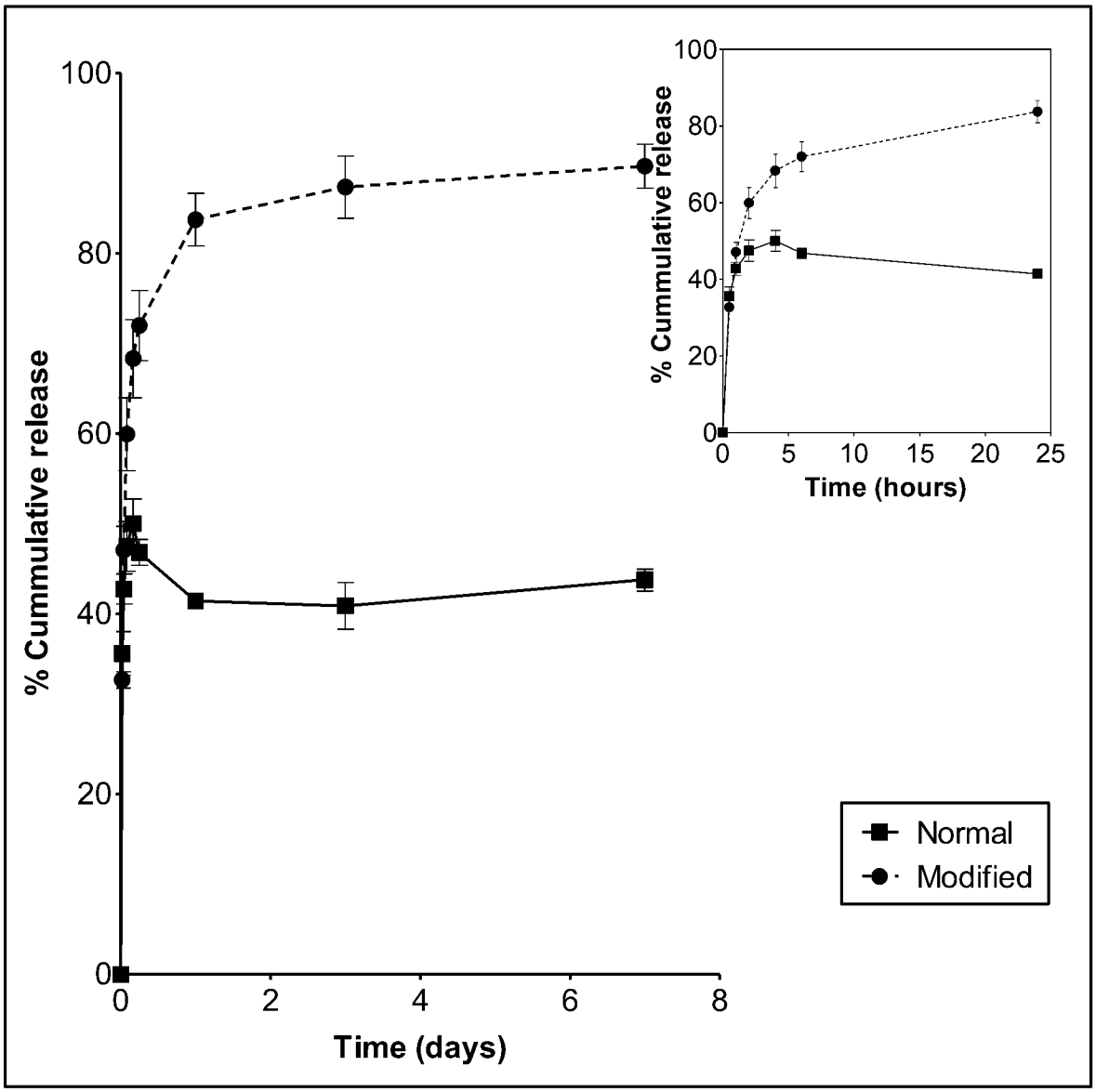

Figure 21: Effect of modified release conditions, on MB release from MB-loaded PHB/PEG (3:2) NFs in PBS pH 7.4 at 37°C for 30 days. Inset: same profile over 24 h (polymer solution concentration 15%w/v)

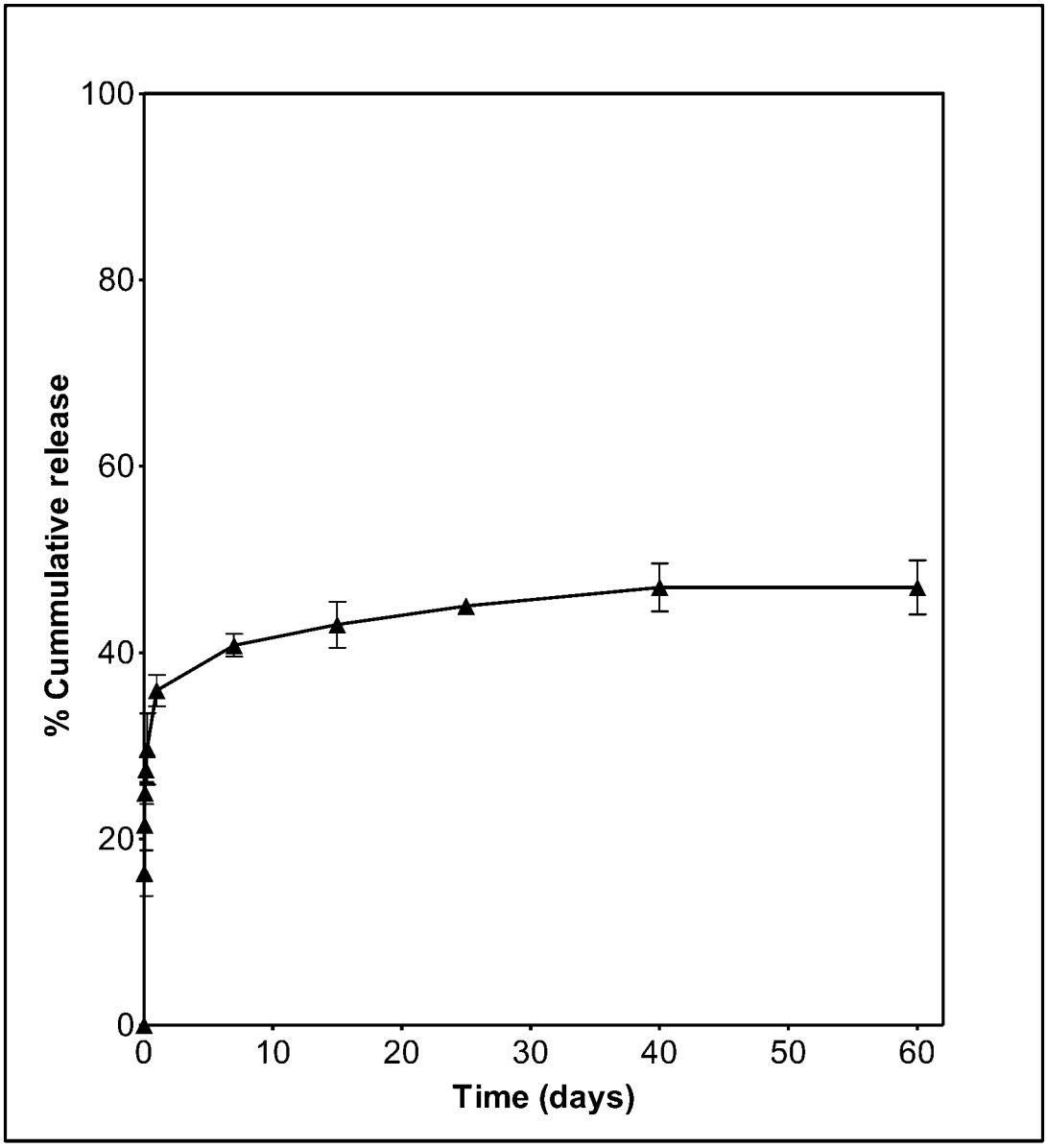

Figure 22: Release profile from MB-loaded PHB NFs over 60 days under modified release conditions in PBS pH 7.4 at 37°C.

3.2.5. Water uptake assessment by selected NFs

One of the main applications intended for the selected PHB-PEG (3:2) formulation is its application as wound dressing for accelerated wound healing. In exuding wounds, excess exudates will predispose the patient to hypergranulation tissue formation in the wound bed and macerate peri-wound skin [277]. Therefore, it is important for a wound dressing to have high capacity for exudates drainage.

A qualitative droplet absorption test was performed by applying a drop of PBS on the surface of MB-loaded PHB and PHB-PEG NFs. Both were then simultaneously photographed (Figure 23). PHB-PEG NFs absorbed the droplet instantly, while PHB NFs took 5 min to absorb the droplet completely. In more quantitative terms, analysis of the water uptake kinetics and capacity of both nanofibrous mats was done by estimating the weight gained by either mats at different time points during incubation in PBS at 37°C (Figure 24). After 15 minutes incubation, the % water uptake was 152 and 272 % for PHB and PHB-PEG NFs respectively. This increased to 180 % and 384 % respectively after 1h incubation. The trends are rather expected due to relatively higher hydrophobicity of PHB. However, considerable water uptake observed for PHB NFs is mediated by the highly porous nature of the NFs. The pores inside nonwoven mats are highly complex in terms of size, shape, and capillary geometry and usually interconnect to form channels that allow water uptake by capillary effect [291, 292]. The water uptake capacity in this case is controlled by the volume of the interconnecting channels. The high water uptake capacity of PHB-PEG NFs is attributed to higher surface hydrophilicity allowing for instant water contact/uptake, and the porogenic effect of PEG [72]. After 24 h, there would be a considerable weight loss in due to leaching of PEG and MB, however the water uptake capacity was still twice that in case of PHB NFs, indicating even higher water uptake that compensated this weight loss. In conclusion, the high water uptake of the developed PHB-PEG NFs is another important criterion supporting potential application of these NFs as a wound dressing material. However, *in vivo* testing remains to prove that the proposed formulation does not cause over-drying of the wound which might interfere with optimal wound healing [293].

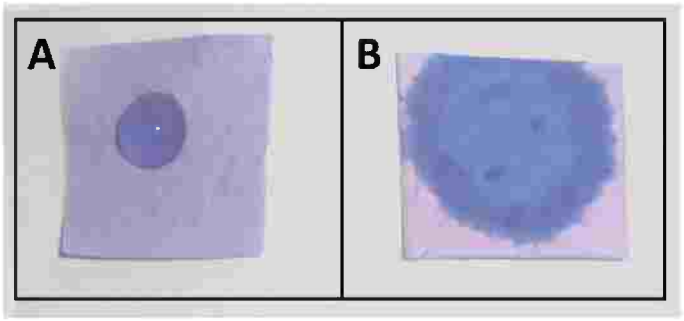

Figure 23: Digital images showing wettability of MB-loaded mats of A) PHB NFs B) PHB/PEG (3:2) NFs.

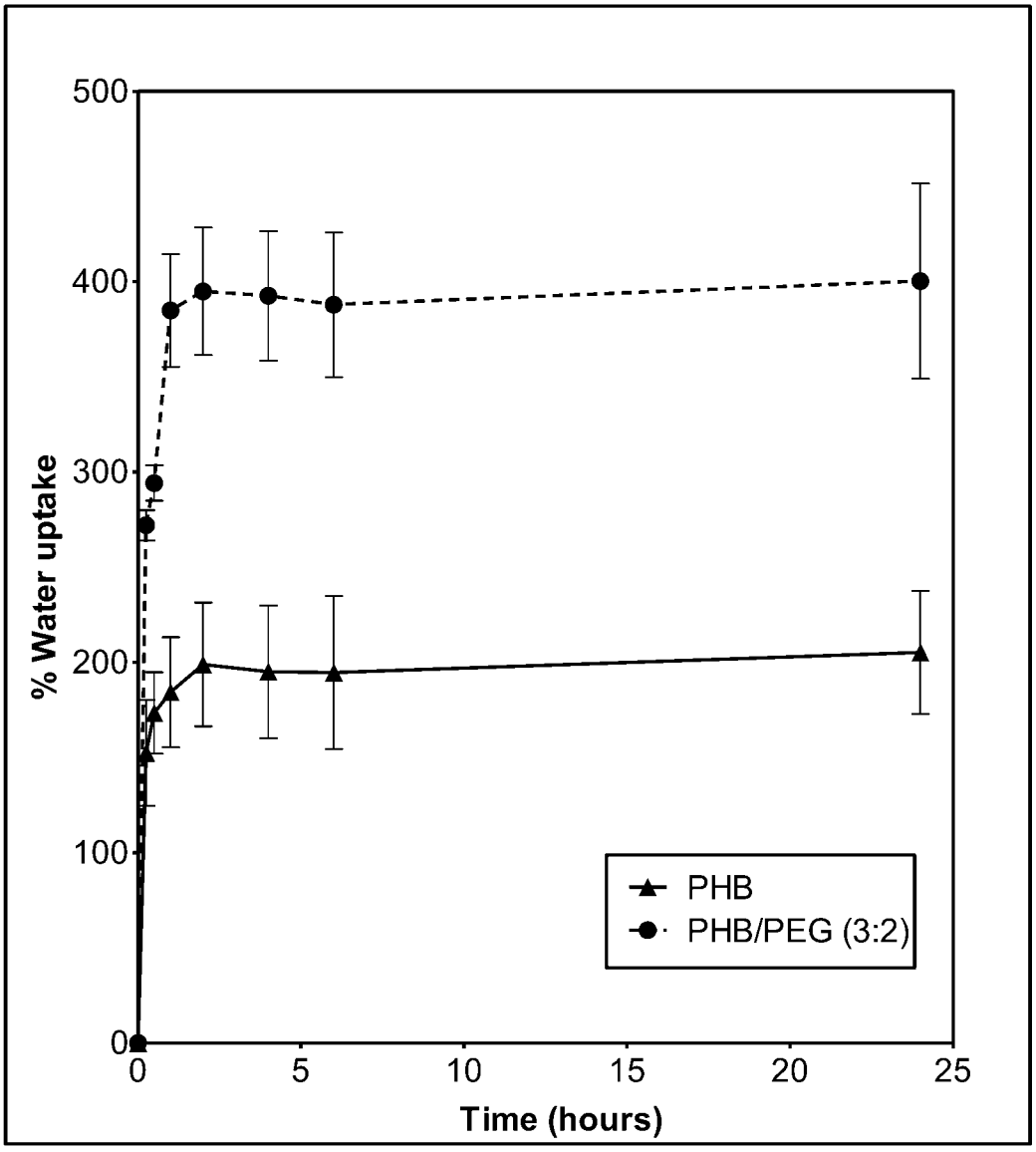

Figure 24: Effect of blending with PEG on water uptake kinetics of MB-loaded PHB NFs in PBS pH 7.4 at 37 °C

3.2.6. *In vitro* degradation of NFs under physiological conditions

Characterization of degradation profiles are critical for optimal application of electrospun fibrous mat as drug carriers, tissue growth scaffolds and wound dressing materials. Generally, polymer matrix degradation is triggered by water absorption into the polymeric bulk. So the type of chemical bond, compositions, molecular organization of the material surface, which influence the surface wettability, as well as the degree of polymer crystallinity and hydrophilicity are the most important factors that influence the velocity of polymer degradation reaction [294].

Figure 25 shows the degradation pattern of both PHB and PHB-PEG (3:2) NFs formulations over 60 days of incubation in PBS at 37°C. PHB NFs showed very little weight loss over the study period. It is known that PHB as hydrophobic, highly crystalline polymer and in this study is also of high Mw, has a relatively slow degradation rate under physiological conditions. Therefore, polymer blending has been frequently used to manipulate its degradation behavior [248, 249]. On the other hand, PHB-PEG (3:2) nanofibrous membranes exhibited significant weight loss up to 30% within only 3 days. This is attributed to the dissolution of PEG molecules nearby the NFs' surface. As PEG could be distributed more deeply in the core, further slower release of PEG proceeded till a weight loss equivalent to the initial PEG loadings (40%) was obtained after 20 days of incubation. Previously, blending PHB with low Mw PEG 300 has been reported to efficiently plasticize PHB membranes due to reduced polymer crystallinity [226]. This was attributed to the interference of PEG with the formation of small PHB spherulites initiating crystallization. In this study, high Mw PEG with more limited chain mobility would not likely interfere with this step; however, since it constitutes 40% of the final blend, it was assumed to decrease the nucleation density during polymer cooling leading to reduction of PHB crystallinity which might promote polymer degradation. No evidence of such effects could be detected at least over this study period since degradation of the remaining matrix was negligible from 20 days onwards.

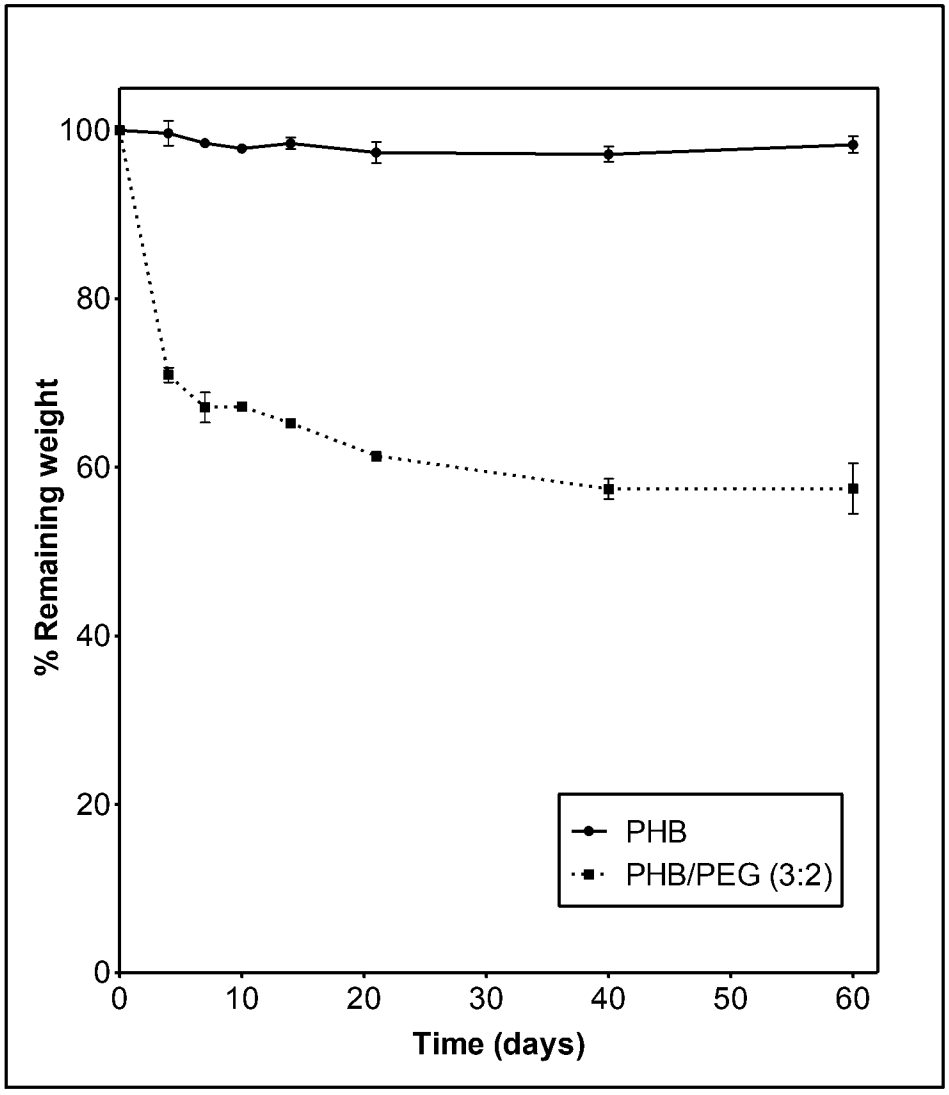

Figure 25: Weight loss of MB-loaded mats of PHB and PHB-PEG (3:2) NFs in PBS pH 7.4 at 37°C using gravimetric analysis

3.2.7. Antibacterial activity

3.2.7.1. Antibacterial activity of MB solution against test organisms

Incubation of two test organisms, Sa_{st} and MRSA, with increasing concentrations of MB resulted in progressive increase in bacterial killing as confirmed by both increase in the % transmittance (%T) and decrease in the survival bacterial count (CFU/ml) (Figures 26 and 27 respectively). Increasing MB concentration to 62.5 µg/ml resulted in increased %T to 90 and 85% for MRSA isolate and Sa_{st} respectively. These values were further enhanced to 98 and 90% respectively at higher MB concentration of 125 µg/ml. The viable count technique showed a similar trend where incubation with 62.5 µg/ml MB resulted in ~ 2.5 $\log_{10}$ CFU reduction in the viable counts of both MRSA and Sa_{st}, which rose to 4 $\log_{10}$ CFU reductions for MRSA upon increasing MB concentration to 125 µg/ml with no more log reduction for Sa_{st}. MB is a cationic phenothiazinium dye previously reported for its antibacterial activity primarily through damage of bacterial cell DNA and to a less extent the outer membrane [295, 296]. The results confirmed susceptibility of both test organisms to MB, and were used for estimation of the antimicrobial activity of MB-loaded NFs.

3.2.7.2. Antibacterial activity of MB-loaded NFs

This experiment was carried out to confirm that the activity of MB was not adversely affected by the electrospinning process. The antibacterial activity of PHB-PEG NFs samples encapsulating ≈ 25 µg MB was compared to that of 50 µl of MB solution (250 and 500 µg/ml) using the agar diffusion method. Figure 28 shows the antibacterial activity of the test groups against Sa_{st} as indicated by the diameter of the inhibition zone. MB solutions used for comparison were of high concentration that could exert high antibacterial activity demonstrated as relatively large inhibition zones, ≈ 29 and 33 mm for 250 and 500 µg/ml respectively. A comparable inhibition zone (≈31) was obtained for the NFs. It should be noted that the amount of MB was equal for both NFs and 500 µg/ml MB solution. Thus, it could be concluded that the developed MB-loaded NFs preserved the antibacterial activity of MB during electrospinning process.

The antibacterial activity of PHB-PEG NFs encapsulating ≈ 5mg MB /g was further investigated against MRSA and Sa_{st} using the viable count technique. Incubation of bacteria with the antibacterial NFs for 1h did not result in a significant killing effect, while after 24 h a 3 and 2.6 $\log_{10}$ CFU reductions were attained for MRSA and Sa_{st} respectively (Figure 29). These values were equivalent to > 99% killing of the initial bacterial population, however, no complete eradication was attained with either test organism. For sound interpretation of these results in confirming the preservation of MB activity during electrospinning, the release profiles of MB from PHB-PEG NFs in the presence of MRSA were obtained under similar experimental settings. The results in Figure 30 showed that MB released in the presence of bacterial population reached ≈ 80 µg/ml after 24 h. The antibacterial effect of the released MB from NFs was, therefore, almost consistent with that of MB solution of equal concentration (Figure 27). Finally, it was noted that a significant antibacterial activity of MB was exerted over 24 h incubation time.

Instantaneous killing effect could be achieved by appropriate light activation of the released MB through photodynamic therapy approach [200].

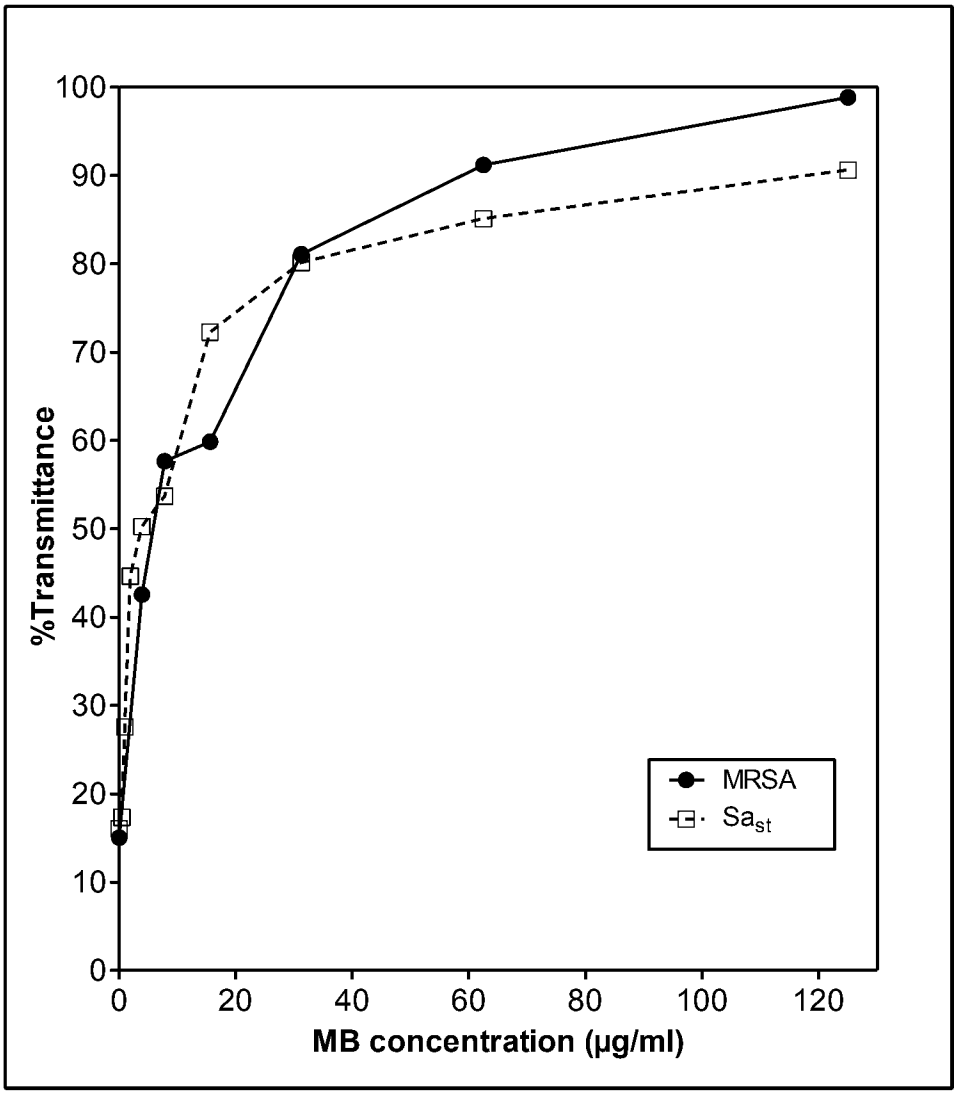

Figure 26: Effect of MB concentration on MRSA and Sa_{st} growth, in terms of % transmittance at 450 nm, upon incubation for 24 h

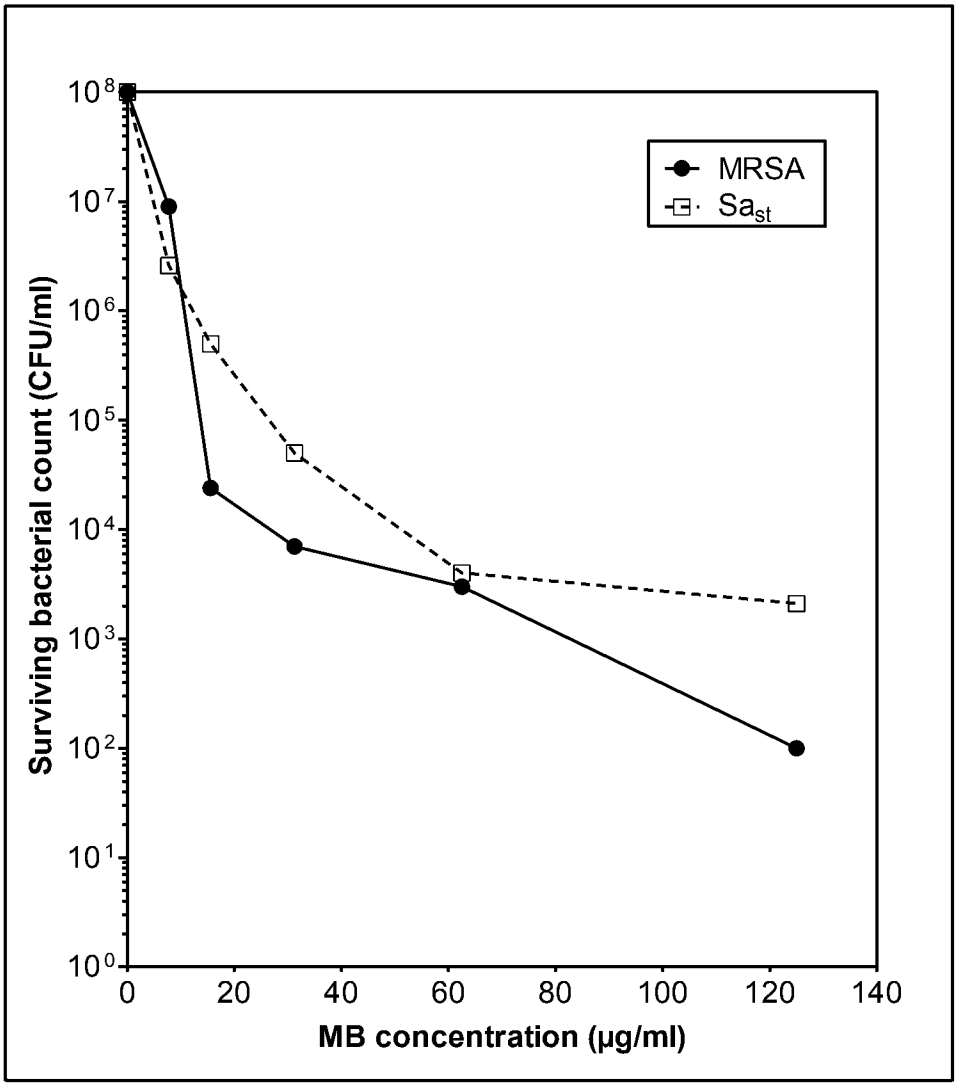

Figure 27: Effect of different MB concentrations on bacterial growth inhibition upon incubation with MRSA and Sa_{st} (~ 10^6 CFU/ml) for 24 h

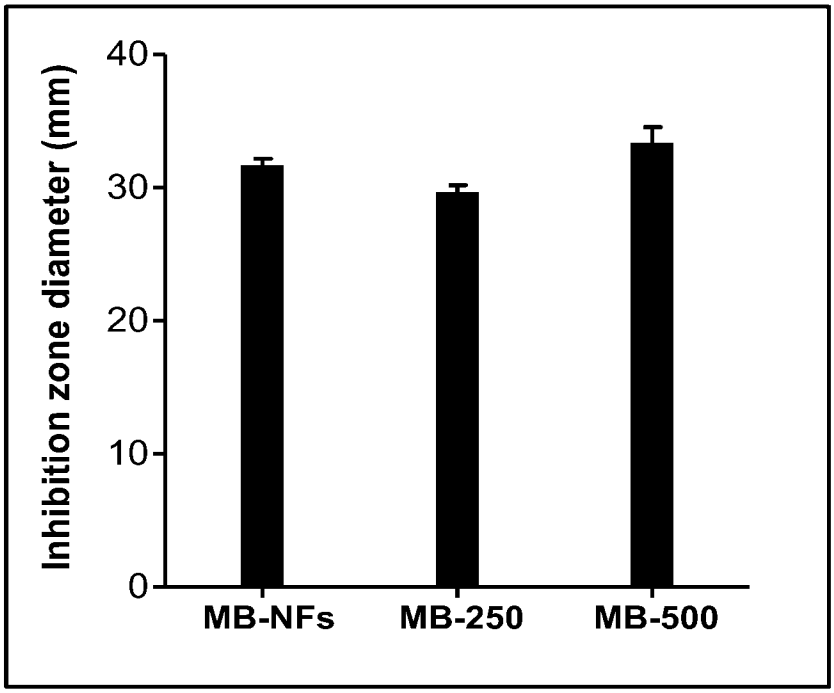

Figure 28: Antibacterial activity of MB-loaded PHB-PEG (3:2) NFs (prepared using 15% polymer solution) in comparison with MB solution (250 and 500µg/ml) against Sa_{st} using the agar diffusion method.

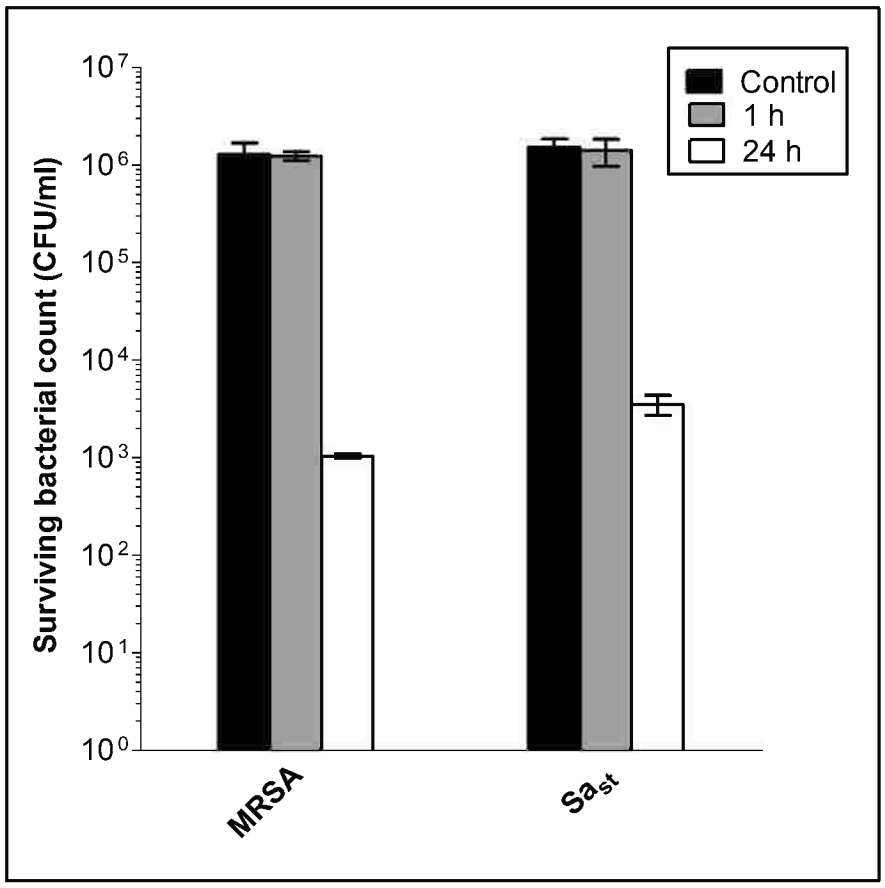

Figure 29: Effect of treatment with MB-loaded PHB/PEG (3:2) NFs (prepared using 15% polymer solution) on the mean surviving bacterial count of 2 bacterial strains; MRSA and Sa_{st} (~ 10^6 CFU/ml), after incubation for 1 and 24 h in the dark, using the viable count technique.

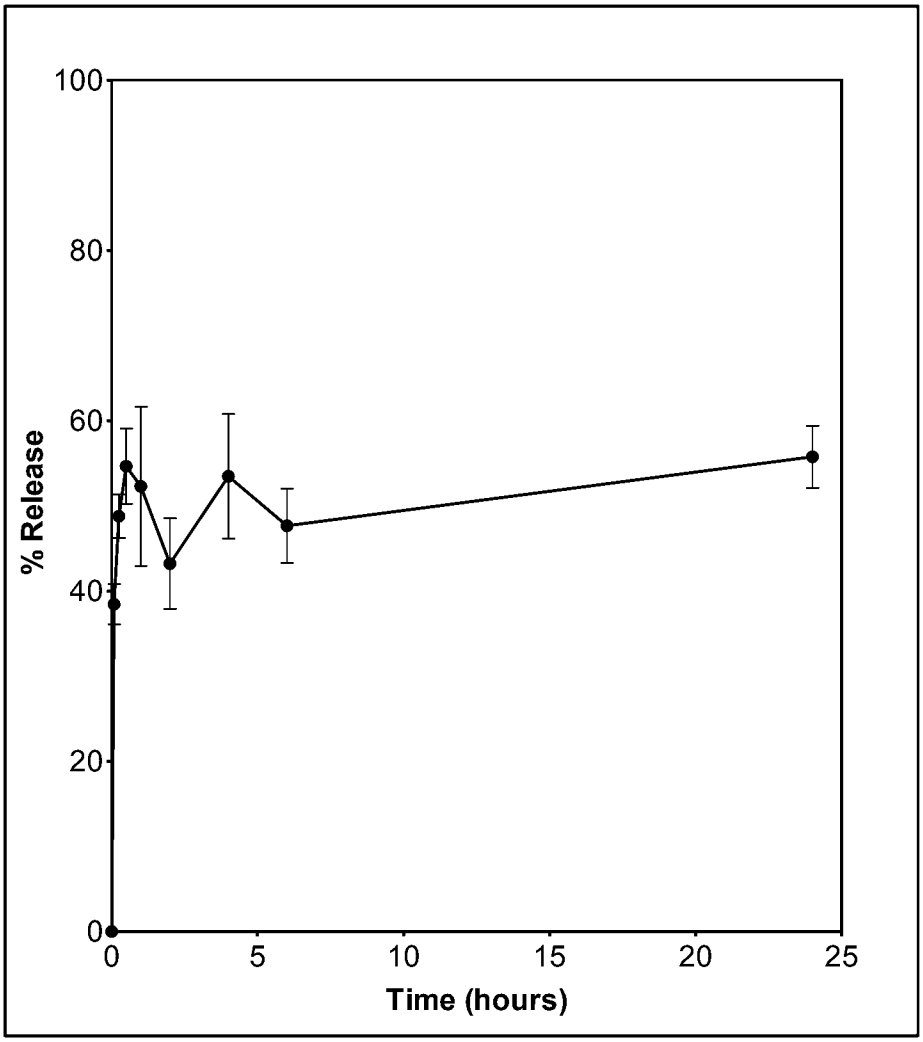

Figure 30: MB release profiles from MB-loaded PHB/PEG (3:2) NFs (prepared using 15% polymer solution) in presence of the test bacterial strain MRSA (~ 10^6 CFU/ml) at 37°C.

4. Conclusion

Novel antimicrobial MB-loaded PHB and PHB-PEG 4000 based NFs have been developed, using the emulsion electrospinning technique, with potential application for different biomedical purposes. The morphology and fiber size of the developed NFs can be controlled by a variety of formulation factors including polymer and PEG concentration. The developed PHB-based NFs with strongly bound MB warrant further investigation as antimicrobial biomaterial with considerable non leaching MB load. PHB-PEG blend NFs allowed tailoring of MB release profiles. PHB-PEG NFs containing 40% PEG 4000 had good formulation attributes suitable for infected wound healing applications because of suitable structural features likely to support enhanced tissue regeneration, high MB initial release rate allowing for significant bacterial killing within 24 h, with further slower release likely to prevent reinfection, and good water uptake capacity in favour of sufficient wound exudates absorption. Further enhancement of the antibacterial effects of the developed NFs through PDT approach is another interesting potential that will be investigated in this thesis. On the other hand, the diversity of MB bio-functions further extends the potentials of the developed systems beyond antimicrobial arena. One possible application to be investigated in this thesis is the potential of the developed NFs in prevention of post-surgical tissue adhesion.